AD-A076 150 ARCON CORP WALTHAM MA F/G 20/14
MATHEMATICAL ANALYSIS AND PROGRAMMING AS APPLIED TO ELECTROMAGN--ETC(U
JUN 79 J O'BRIEN , I KOLTUNOV F19628-76-C-0310
UNCLASSIFIED RADC-TR-79-146 NL

1 OF 2
AD
A076150

RADC-TR-79-146
Final Technical Report
June 1979

LEVEL II

MATHEMATICAL ANALYSIS AND PROGRAMMING AS APPLIED TO ELECTROMAGNETIC PROPAGATION AND ANTENNA DESIGN

ARCON Corporation

John O'Brien
Ilya Koltunov
Peter Wintersteiner
Ben-Zion Guz

ROME AIR DEVELOPMENT CENTER
Air Force Systems Command
Griffiss Air Force Base, New York 13441

This report has been reviewed by the RADC Information Office (OI) and is releasable to the National Technical Information Service (NTIS). At NTIS it will be releasable to the general public, including foreign nations.

RADC-TR-79-146 has been reviewed and is approved for publication.

APPROVED: Walter Rotman

WALTER ROTMAN, Chief
Antennas and RF Components Branch
Electromagnetic Sciences Division

APPROVED: Allan C. Schell

ALLAN C. SCHELL, Chief
Electromagnetic Sciences Division

FOR THE COMMANDER: John P. Huss

JOHN P. HUSS
Acting Chief, Plans Office

If your address has changed, or if you wish to be removed from the RADC mailing list, or if the addressee is no longer employed by your organization, please notify RADC (EEA), Hanscom AFB MA 01731. This will assist us in maintaining a current mailing list.

Do not return this copy. Retain or destroy.

UNCLASSIFIED

SECURITY CLASSIFICATION OF THIS PAGE (When Data Entered)

REPORT DOCUMENTATION PAGE	READ INSTRUCTIONS BEFORE COMPLETING FORM
1. REPORT NUMBER: RADC-TR-79-146	2. GOVT ACCESSION NO. / 3. RECIPIENT'S CATALOG NUMBER
4. TITLE (and Subtitle): MATHEMATICAL ANALYSIS AND PROGRAMMING AS APPLIED TO ELECTROMAGNETIC PROPAGATION AND ANTENNA DESIGN	5. TYPE OF REPORT & PERIOD COVERED: Final Technical Report, 28 Sep 76 — 30 Jun 78
	6. PERFORMING ORG. REPORT NUMBER: N/A
7. AUTHOR(s): John O'Brien, Peter Wintersteiner, Ilya Koltunov, Ben-Zion Guz	8. CONTRACT OR GRANT NUMBER(s): F19628-76-C-0310
9. PERFORMING ORGANIZATION NAME AND ADDRESS: ARCON Corporation, 260 Bear Hill Road, Waltham MA 02154	10. PROGRAM ELEMENT, PROJECT, TASK AREA & WORK UNIT NUMBERS: 61102F, 99930000
11. CONTROLLING OFFICE NAME AND ADDRESS: Deputy for Electronic Technology (RADC/EEA), Hanscom AFB MA 01731	12. REPORT DATE: June 1979
	13. NUMBER OF PAGES: 95
14. MONITORING AGENCY NAME & ADDRESS (if different from Controlling Office): Same	15. SECURITY CLASS. (of this report): UNCLASSIFIED
	15a. DECLASSIFICATION/DOWNGRADING SCHEDULE: N/A

16. DISTRIBUTION STATEMENT (of this Report)

Approved for public release; distribution unlimited

17. DISTRIBUTION STATEMENT (of the abstract entered in Block 20, if different from Report)

Same

18. SUPPLEMENTARY NOTES

RADC Contract Monitor: John McIlvenna (EEA)

19. KEY WORDS (Continue on reverse side if necessary and identify by block number)

Magneto-acoustic Surface Waves	Ionospheric Pulse Reflections
Propagation through Multiple Layers	Target Tracking
Detection of Signals	Arrested Synthetic Aperature
Clutter and Noise	Signal Spectrum
Polar VLF Propagation	Loran

20. ABSTRACT (Continue on reverse side if necessary and identify by block number)

In this report, the analysis and programming for various problems in the field of Electromagnetic propagation and antenna design are considered.

The scope of our work extended into a variety of technical areas. Among the technical areas are:

(1) Magneto-acoustic surface waves → next page

(Cont'd on reverse)

DD FORM 1 JAN 73 1473

UNCLASSIFIED

SECURITY CLASSIFICATION OF THIS PAGE (When Data Entered)

403370

(2) Signal analysis,

(3) Polar VLF propagation,

(4) Ionospheric pulse reflections,

(5) Detection and tracking of targets, and

(6) Antenna Design.

EVALUATION

The topics covered in this report represent a collection of specialized mathematical and programming problems encountered in the antenna and propagation research at RADC/EE during the 1976 to 1978 time period. All the problems required detailed mathematical analysis and computer programming for solution. The report summarizes the several problem areas, presents the basic equations and points out the highlights of the resulting computer programs.

John F. McIlvenna

JOHN F. MCILVENNA
Contract Monitor

PREFACE

The computer programs and results herein are the result of analytical research performed for:

Deputy for Electronic Technology (RADC/ET)
Air Force Systems Command, USAF
Hanscom Air Force Base, Massachusetts 01731

TABLE OF CONTENTS

TABLE OF CONTENTS (Cont'd)

TABLE OF CONTENTS (Cont'd)

TABLE OF CONTENTS (Cont'd)

TABLE OF CONTENTS (Cont'd)

I. INTRODUCTION

During the past two years, we have worked on several tasks in a variety of areas.

Analytical and computational support was provided in the development of a theoretical basis for the generation, detection and processing of microwave magnetostatic surface wave signals using periodic structures.

A program was written to analyze the diffraction of an incident, linearly polarized plane wave at arbitrary incident angle by one or several metal strip grids.

A program was written to evaluate some multiple integrals having to do with the detection of radar signals in the presence of background noise and ground clutter.

Programing was done to produce a computer-drawn map of the earth, or a certain portion of the earth.

Programing support was given to ongoing research involving continuous measurements of many ionospheric and atmospheric parameters.

Modifications were made to an existing program which had been written to calculate the effects of different model ionospheres on VLF signals reflected from them.

A computer model has been developed to simulate the performance of a ground based radar so as to include the effects of terrain screening,

bird clutter, ground clutter, Raleigh distributed noise, multipath and surface roughness.

A program was written that computes the improvement factor for the arrested synthetic aperture radar.

In conjunction with the Loran problem, a program was written to compute the spectrum of an ensemble of signals.

Finally, analysis and programming was done for the maximazation of gain of a wire antenna.

II. ANALYTICAL AND COMPUTATIONAL TECHNIQUES FOR THE ANALYSIS OF PERIODIC MAGNETOACOUSTIC SURFACE WAVES

1. Introduction

We have been privileged to provide collaborative effort in the analytical areas of numerical and computational support in the development of a theoretical basis for the generation/detection and processing of microwave magnetostatic surface wave (MSSW) signals using periodic structures.

This work describes the interaction of magnetic surface waves with multiple and periodic conductors carrying nonuniform currents. In addition, a double ground plane structure is included in the analysis, and expressions are derived for radiation resistance and space harmonic amplitudes. The results are applicable to the advanced design of magnetostatic surface wave filters and delay lines.

2. Statement of the Problem

A transducer in the form of a meander line or grating, such as shown in Fig. I-1 is excited with RF current. Fig. I-2 illustrates how the transducer is connected to the ground plane structure and to the input/output line. The current sets up magnetic fields which generate a variety of propagating modes within the structure. One particular mode has a high potential for sophisticated signal applications at microwave frequencies. The mode known as a magnetostatic surface wave, MSSW, has the following characteristics: it is non-reciprocal; propagates perpendicular to a magnetic biasing field and is guided by two parallel surfaces. Most of its energy is concentrated near one surface; it propagates with a velocity between that of acoustic and light

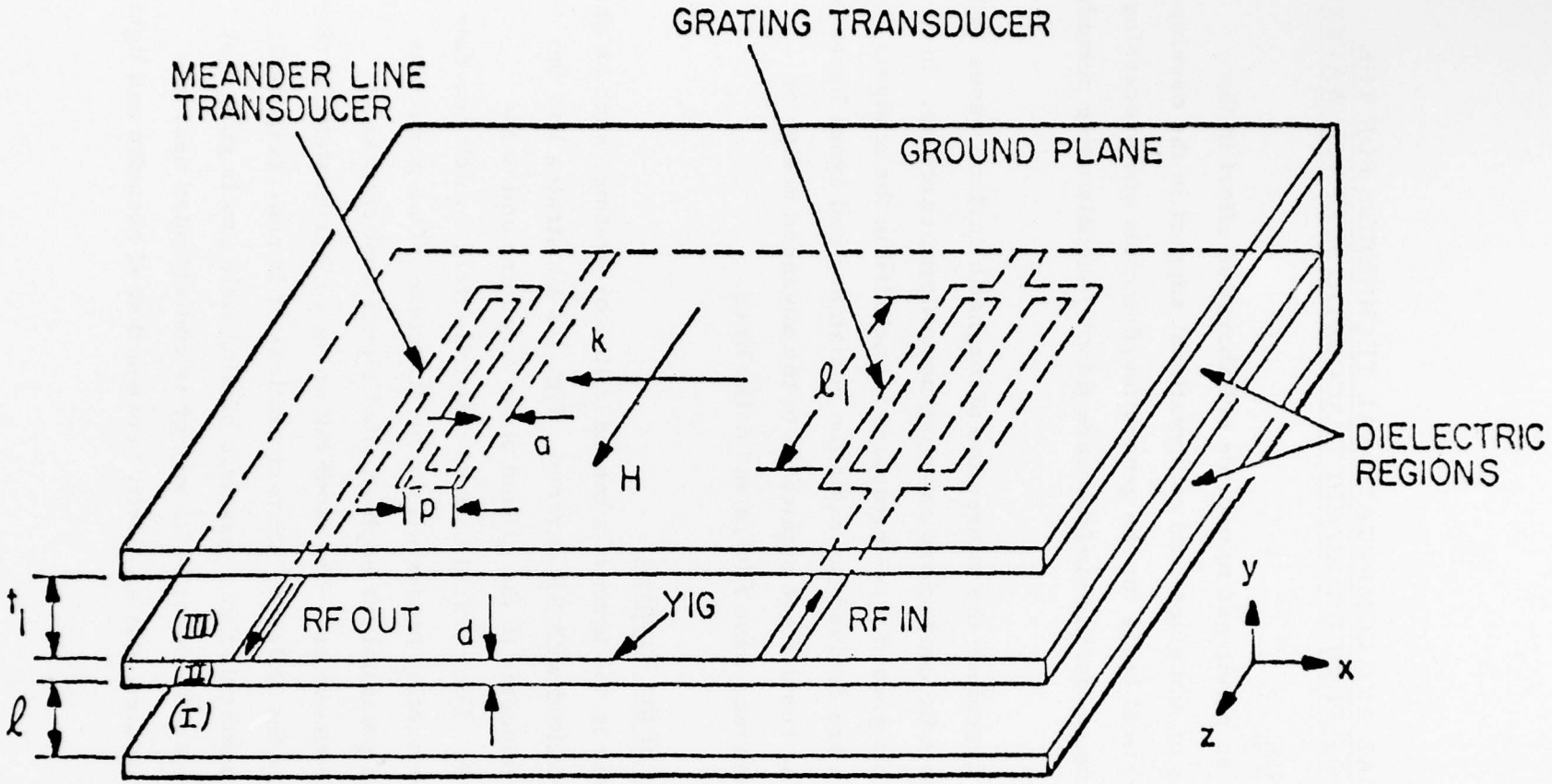
GRATING TRANSDUCER
MEANDER LINE TRANSDUCER
GROUND PLANE
k
a
H
p
ℓ_1
DIELECTRIC REGIONS
t_1
(III)
RF OUT
d
YIG
RF IN
(II)
ℓ
(I)
y
x
z

Fig. 1-1

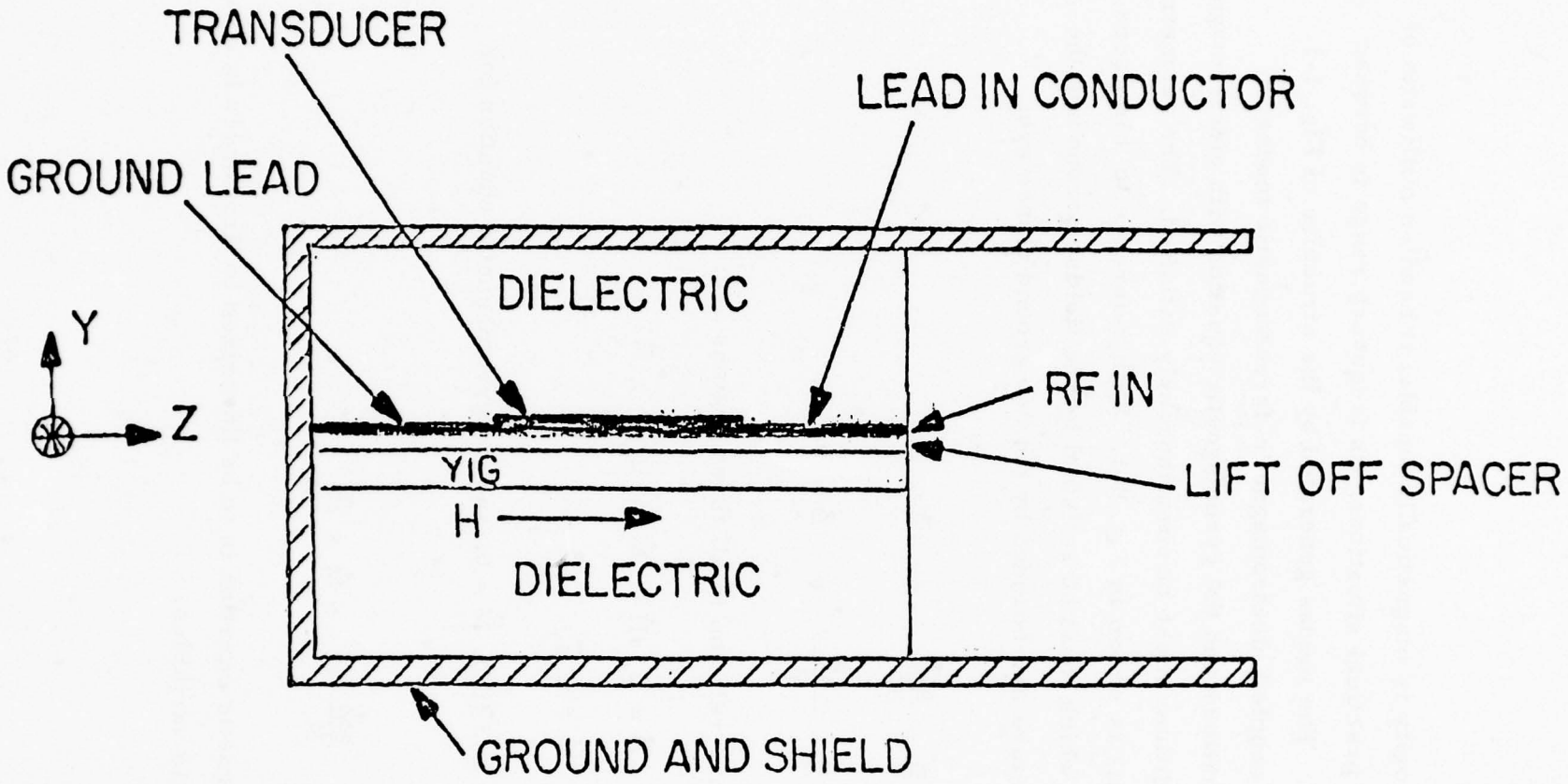
TRANSDUCER
LEAD IN CONDUCTOR
GROUND LEAD
DIELECTRIC
Y
Z
RF IN
YIG
LIFT OFF SPACER
H
DIELECTRIC
GROUND AND SHIELD

Fig. I-2

waves; its velocity is magnetically tunable; it handles milliwatts of power; and in practical situations, its frequency range is between 2 and 20 GHZ. The modes generated by the structure of Fig. I-1. are basically coupled electromagnetic-ferromagnetic modes. Maxwell's equations and the gyromagnetic equation with electromagnetic boundary conditions must be simultaneously satisfied. The geometry for the analysis is shown in Fig. I-1. With reference to this figure, the equations which must be satisfied by the fields surrounding the periodic structure and bounded by the two ground planes are:

$$\nabla \times \vec{H} = \frac{\partial \vec{D}}{\partial t} \quad , \quad \nabla \cdot \vec{B} = 0$$

$$\nabla \times \vec{E} = \frac{-\partial \vec{B}}{\partial t} \quad , \quad \nabla \cdot \vec{D} = 0 \tag{1}$$

The constitutive relation in all three regions are:

$$\vec{B} = \mu_o (\vec{H} + \vec{M}) = \mu_o \overleftrightarrow{\mu}_\gamma \cdot \vec{H}$$

$$\vec{D} = \epsilon_o \overleftrightarrow{\epsilon}_r \cdot \vec{E} \tag{2}$$

In regions (I) and (III), $\vec{M} = 0$, and the gyromagnetic equation for region (II) is:

$$\frac{\partial \vec{M}}{\partial t} = - \gamma \vec{M} \times \vec{H} \tag{3}$$

This gyromagnetic equation is to be linearized to first order in small signal RF field variables.

3. Transverse Electric (TE) Modes

Maxwell's equations can be separated into two sets of equations: one set for E_x, E_y, and H_z (the transverse magnetic or TM mode), and one set for E_z, H_x, and H_y (the TE mode). TE mode solutions are characterized by the following conditions: $\partial/\partial z \to 0$ for all fields and the wave solutions have the form

$$f_k(y) \exp [i(\omega t - kx)]$$

where $$f_k(y) = A_{kR} \exp(ky) + B_{kR} \exp(-ky)$$

for every region R (Fig. I-1). The magnetic biasing field H is Z directed. The nonzero field components satisfy the following reduced equations.

$$\frac{\partial H_y}{\partial x} - \frac{\partial H_x}{\partial y} = i\omega\epsilon E_z \tag{4}$$

$$\frac{\partial E_z}{\partial y} = -\omega B_x$$

$$\frac{\partial E_z}{\partial x} = i\omega B_y \tag{5}$$

$$\frac{\partial B_x}{\partial x} + \frac{\partial B_y}{\partial y} = 0 \tag{6}$$

The $\nabla \cdot \vec{D}$ equation is automatically satisfied since $E_x = E_y = 0$ and $\partial/\partial z \to 0$. The magnetization vector has the form

$$\vec{M} = M_x X + M_y Y + M_o Z$$

and the linearized magnetization equation reduces to:

$$\begin{aligned} i\omega M_x &= \gamma M_o H_y - \gamma H_o M_y \\ i\omega M_y &= \gamma M_o H_x + \gamma H_o M_x \end{aligned} \tag{7}$$

Using $\vec{B} = \mu_o (\vec{H} + \vec{M})$ and the preceding equations,

$$\begin{pmatrix} B_x \\ B_y \end{pmatrix} = \mu_o \begin{pmatrix} \mu_{11} + i\mu_{12} \\ -i\mu_{12} \quad \mu_{22} \end{pmatrix} \begin{pmatrix} H_x \\ H_y \end{pmatrix} \tag{8}$$

The solutions for B_y and H_x in each of three regions are given as integrals of functions $f_k(y) = A_{kR} \exp(ky) + B_{kR} \exp(-ky)$, where R is the number of the region.

The electric field E_z in each of the three regions is obtained by multiplying the integrand of B_y by $(-\omega/k)$. H_y and B_x are obtained from B_y and H_x from the permeability matrix (8).

All of the field equations and the final power expression are valid for anisotropic media. For the isotropic case

$$\mu_{11} = \mu_{22} = 1 - \frac{\Omega_H}{\Omega^2 - \Omega_H^2}$$

$$\mu_{12} = \frac{\Omega}{\Omega^2 - \Omega_H^2} \quad , \quad \Omega_H = H/(4\pi M_o) \tag{9}$$

$$\Omega = \frac{\omega}{\gamma \cdot 4\pi M_o} \quad \text{and} \quad \begin{matrix} \gamma = 2.8 \text{ MHZ/oersted} \\ 4\pi M_o = 1750 \text{ oersted} \end{matrix}$$

4. Boundary Conditions

In order to solve the equations of the preceding section and evaluate the constants A_{kR}, B_{kR} the following boundary conditions apply. With reference to Fig. I-1,

$$\begin{aligned} B_y &= 0 \text{ at } y = t_1 \text{ and } y = -(d + \ell) \\ B_y^{I} &= B_y^{II} \text{ at } y = -d \\ B_y^{II} &= B_y^{III} \text{ at } y = 0 \\ H_x^{I} &= H_x^{II} \text{ at } y = -d \end{aligned} \tag{10}$$

The boundary condition due to current in the periodic structure is

$$H_x^{III} - H_x^{II} = J(x) \text{ at } y = 0 \tag{11}$$

All coefficients are given in terms of a Fourier transform of an arbitrary surface current distribution J(x).

This is an important result because it provides a procedure for sophisticated transducer designs. For example, non-periodic (or periodic) conducting strips may be driven with independent current sources; then an integration (or Fourier transform) over the source distribution provides a quick determination of all important transducer characteristics.

5. General Fields and the Characteristic Equation

To obtain the total fields in the three regions, which are integrals, use of residue theory is required.

The characteristic relationship between frequency and wave number for the unelectroded structure, consisting of YIG slab and both ground planes, is given by

$$F_T(k, \omega) = \beta_3(\alpha_2 e^{-2\beta_2 |k| d} - \alpha_1 T) \coth(\beta_3 |k| t_1) - (e^{-2\beta_2 |k| d} + T) = 0,$$

OR

$$e^{-2\beta_2 / k/d} = \frac{T[\alpha_1 \beta_3 \coth(\beta_3 |k| t_1) + 1]}{[\alpha_2 \beta_3 \coth(\beta_3 |k| t_1) - 1]} , \tag{12}$$

where

$$\alpha_{1,2} = \frac{\mu_{11}\mu_{22} - \mu_{12}^2}{\mu_{11}\beta_2 \pm \mu_{12} S} ,$$

$$T = \frac{\alpha_2 + 1/\beta_1 \tanh(\beta_1 |k| \ell)}{\alpha_1 - 1/\beta_1 \tanh(\beta_1 |k| \ell)} ,$$

and

$$S = \pm 1.$$

6. Magnetostatic Surface Solutions

In the magnetostatic limit, MSSW wavelengths are much smaller than electromagnetic wavelengths in regions of dielectric constant ϵ. That is, $\lambda_s \leq \lambda_\epsilon$. This is equivalent to

$$k_s \gg \sqrt{\epsilon}\, \omega / c_o = k^o_\epsilon$$

For $\omega = 2\pi \times 3 \times 10^9 \text{ sec}^{-1}$, $c_o = 3 \times 10^8$ m/sec , (13)

and $\epsilon = 10$. It was found that $k^o_\epsilon \approx 2 \text{ cm}^{-1}$ or $\lambda^o_\epsilon \approx \pi$ cm.

This means MSSW wavelengths up to a few thousand microns satisfy inequality (13) very well. Practical MSSW wavelengths are on the order of hundreds of microns and so (13) is well satisfied in practice.

For a given frequency ω, k is found from the characteristic equation

$$F_{TM} = F_T\Big|_{k \gg k_\epsilon^o} = (\alpha_2 e^{-2\beta|k|d} - \alpha_1 T_M) \coth(|k|t_1) - (e^{-2\beta|k|d} + T_M) ,$$

Where $\beta = \sqrt{\mu_{22}/\mu_{11}}$ (14)

$$T_M = \frac{\alpha_2 + \tanh(|k|\ell)}{\alpha_1 - \tanh(|k|\ell)} .$$

7. MSSW Fower

From the $\nabla \times \vec{E} = -\vec{B}$ equation,

$$E_z^{(s)} = -S(\omega/k)\, B_y^{(s)} \tag{15}$$

and from the permeability matrix, (8)

$$H_y^{(s)} = 1/\mu_{22} \left(\frac{B_y^{(s)}}{\mu_o} + i\mu_{12} H_x^{(s)} \right) \tag{16}$$

The power density carried by a MSSW in the x direction is

$$P^{(s)} = 1/2\, E_z^{(s)} H_y^{(s)} \tag{17}$$

while total power, for width ℓ_1, is

$$P^{(s)} = \frac{e_1}{2} \int_{-(\ell + d)}^{t_1} E_z^{(s)} \cdot H_y^{(s)} dy \qquad (18)$$

After substitution of $B_y^{(s)}$, $H_x^{(s)} F_{TM}$, E_z and $H_y^{(s)}$ into $P^{(s)}$, a final expression for P is

$$P^{(s)} = \frac{\omega \mu_o \ell_1}{2k_s^2} \left| G(k, \omega) \right|^2 \left| A(k_s) \right|, \qquad (19)$$

Where

$$A(k_s) = (T_M + 1) \left[\frac{\frac{\text{Sinh } (2k_s \ell)}{4} - \frac{k_s \ell}{2}}{\text{Cosh}^2 (k_s \ell)} \right] + (\alpha_1 T_M e^{\beta k_s d} -$$

$$- \alpha_2 e^{-\beta k_s d)^2} \cdot \left[\frac{\frac{\text{Sinh } (2k_s t_1)}{4} - \frac{k_s t_1}{2}}{\text{Sinh}^2 (k_s t_1)} \right] + \frac{\alpha_1}{2} T_M^2 (e^{2\beta k_s d} - 1) -$$

$$- \frac{\alpha_2}{2} (e^{-2\beta k_s d} - 1) - 2k_s d T_M \mu_{11} .$$

In evaluating power, (19), $k_s = |k|$ satisfying $F_{TM} = 0$ from (14), and

$$G(k, \omega) = \frac{\mathfrak{I}(S \cdot k_s) \, e^{-\beta k_s d}}{F_{TM}^{(1)} (k_s, \omega)} . \qquad (20)$$

8. Radiation Resistance

In this section are given expressions for radiation resistance of a meander and grating line transducer assuming uniform current distribution in each conductor.

A transducer is made up of N conducting strips each of width "a" carrying current I_o.

When $\eta = +1$ all conductors are connected in parallel to form a grating, and when $\eta = -1$ they are connected in series to form a meander line.

After taking the Fourier transform of this current distribution and substitution into (19) and (20), the radiation resistance, $R_m^{(s)}$, can be obtained as follows:

$$P^{(s)} = 1/2\, R_m^{(s)} \cdot \left|I_T\right|^2 , \tag{21}$$

Where $I_T = I_o/2\,[(1 - \eta) + (1 + \eta)\, N]$

and $$R_m^{(s)} = \frac{2R_o^{(s)}}{[(1-\eta) + (1 + \eta)\, N^2]} \left[\frac{\mathrm{Sin}\,(a\, k_s/2)}{(a\, k_s/2)}\right]^2 \left|\frac{1 - \eta^N e^{ikpN}}{1 - \eta e^{ikp}}\right|^2 , \tag{22}$$

and $$R_o^{(s)} = \frac{\omega \mu_o e_1 e^{-2\beta k_s d}}{k_s^2 \left|F_{TM}^{(1)}(k_s, \omega)\right|^2} \left|A(k_s)\right|$$

Then for a grating, $\eta = +1$,

$$R_m^{(s)} = \frac{R_o^{(s)}}{N^2} \left[\frac{\mathrm{Sin}\,(ak_s/2)}{(ak_s/2)}\right]^2 \left[\frac{\mathrm{Sin}\,(k_s pN/2)}{\mathrm{Sin}\,(k_s p/2}\right]^2 \tag{23}$$

For a meander line, $\eta = -1$, with N even,

$$R_m^{(s)} = R_o^{(s)} \left[\frac{\mathrm{Sin}\,(a\, k_s/2)}{(a\, k_s/2)}\right] \left[\frac{\mathrm{Sin}\,(k_s p\, N/2)}{\mathrm{Cos}\,(k_s p/2)}\right]^2 \tag{24}$$

Fig. I-3 gives curves of total radiation resistance per unit width, $(R_m^{(+)} = R_m^{(-)})/\ell_1$, for the single strip case, N = 1. $R_m^{(+)}$ and $R_m^{(-)}$ are obtained using equation (22). For all curves, a = 178 μm, H = 650 oe and d = 6.25 μm.

9. Computational Techniques and Numerical Analysis

Program EXC has been developed to effect numerical analysis in order to test the general design theory for magnetostatic surface wave periodic transducer structures; analyze the behavior of the functions P and R; obtain an accurate correspondence between theory and experiment; and compare the results thus obtained with those of other investigators. This testing and analysis consists of performing the following functions:

Plotting Dispersion Diagram for $\Omega = f(k)$ for both $F_T(k, \omega) = 0$ $(S = \pm 1)$, and $F_{TM}(k, \omega) = 0$ $(S = \pm 1)$.

Calculation of the power carried by MSSW P_+ $(S = 1)$ and P_- $(S = -1)$.

Analysis of the behavior of the power and Radiation Resistance functions in the neighborhood of a given frequency ω_o and plotting the graphs of these functions.

Evaluation of the power generated as a function of width to half period ratio (a/p).

To carry out the functions mentioned above, Program EXC calculates the roots of transcendental equations $F_{TM}(k, \omega) = 0$ and $F_T(k, \omega) = 0$ for every given frequency ω relating wave number k.

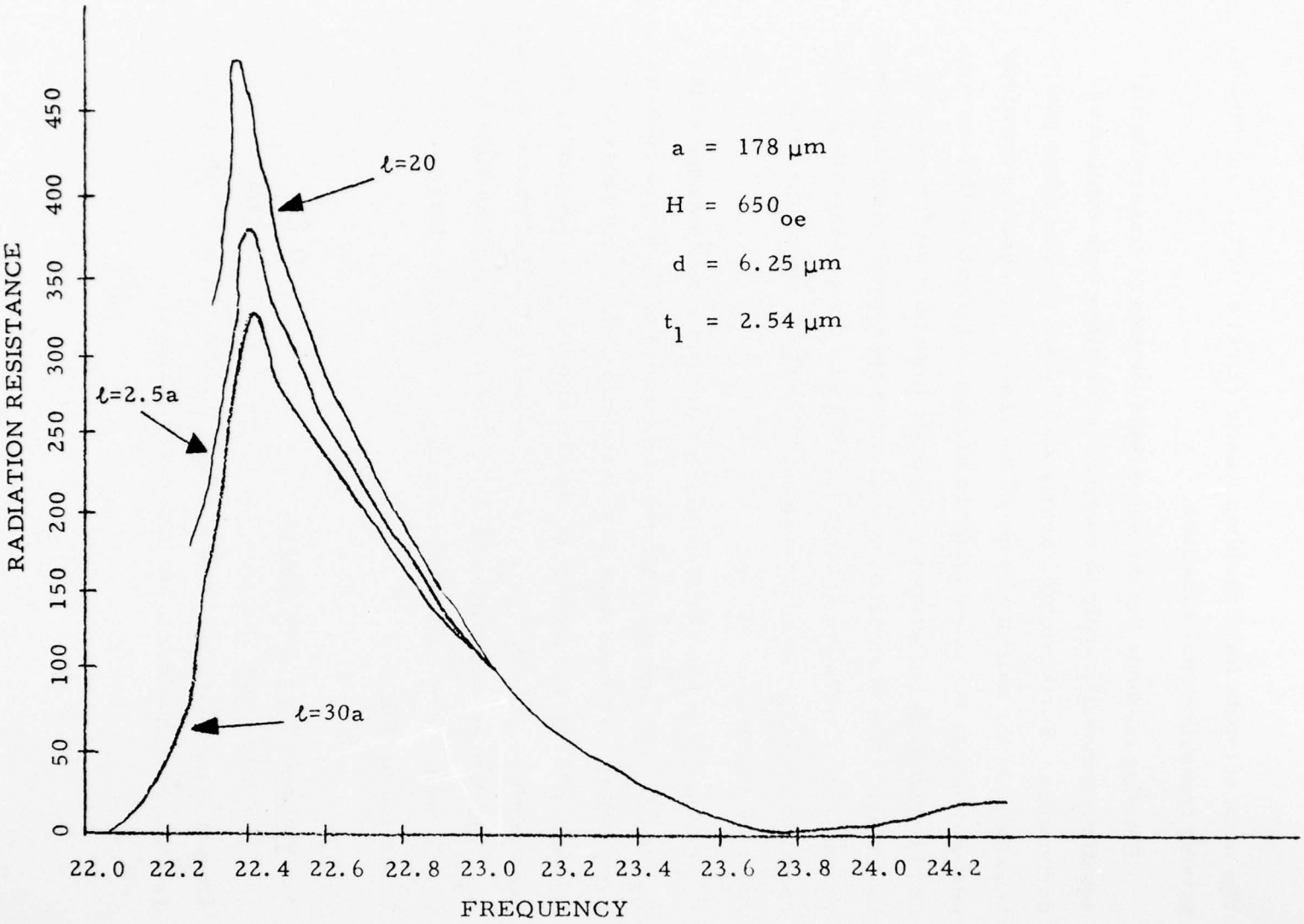
RADIATION RESISTANCE
0
50
100
150
200
250
300
350
400
450
22.0
22.2
22.4
22.6
22.8
23.0
23.2
23.4
23.6
23.8
24.0
24.2
FREQUENCY
ℓ=20
ℓ=2.5a
ℓ=30a
a = 178 μm
H = 650 oe
d = 6.25 μm
t1 = 2.54 μm

Fig. I-3

The main computational problem was to select a suitable method for solving transcendental equations.

Existing methods for the numerical solution of transcendental equations generally apply to continuous functions with continuous derivatives. Furthermore, nearly all of them require some prior knowledge of the neighborhoods of the roots. Because the functions associated with the above analysis are not in general well-behaved, and because it is sometimes impossible to predict all the root locations, it has been necessary to make appropriate modifications to the Mueller iteration scheme.[6] This was done by insertion of the condition at infinity for transcendental functions within the given range of argument.

On the other hand, subroutine RTMI requires knowledge of the $X_{\ell i}$ and X_{ri} left and right bounds of the range of X, where unknown roots exists. To overcome this restriction, the whole range of frequency (or wave number) is divided into n equal segments, for each of which, DISCR = $X_{\ell i} \cdot X_{ri}$ is calculated. That pair of $X_{\ell i}$ and X_{ri}, which gives a negative value of DISCR, are left and right bounds for the root. For oscillating functions, n should be large (from 100 to 300).

A. Plotting Dispersion Diagram

The Dispersion Diagram was plotted. For each value of frequency ω, the equations FT(k, ω) = 0, FTM (k, ω) = 0 were solved relating wave number k for both cases (S = $\pm$ 1).

B. Calculation of the Power Carried by MSSW

The calculation of the power carried by MSSW (P_+ and P_-) was realized by means of subroutine POW, varying frequency ω for given S. The value k, which occurs in the function POW, is calculated using subroutines RTMI and FTM.

C. Plotting the Graph of the Radiation Resistance

Plots of the Radiation Resistance as a function of frequency were performed on the CDC6600 on-line plotter. The frequency range is given, the number of arguments varies depending on the goal of the analysis; k-values are the same as for power calculation. The range of frequency is not divided into equal segments because in the neighborhood of the peak, (ω_o = 3.56 GHZ) the function is rapidly increasing and more points are needed.

D. Evaluation of the Power Generated as a Function of the Parameters

The power (or Radiation Resistance) is very sensitive to variation in the parameters. Variation of the parameters a, ℓ, t_1 must be in the range over which the function exists (Fig. I-3). For example, with the parameters given in the Figure, the junction (Radiation Resistance) does not exist below about 22×10^9 radians/sec. or 3.5 GH_z.

2. REFERENCES

1. Sethares, J., Tsai, T. and Koltunov, I., Periodic Magnetostatic Surface Wave Transducers, RADC-TR-78-78, Rome Air Development Center, Griffiss Air Force Base. AD# A057 214.

2. Ganguly, A.K. and Webb, D.C. (1975) Microstrip Excitation of Magnetostatic Surface Waves: Theory and Experiment, IEEE Transactions on Microwave Theory and Techniques. Vol. MTT-23, No. 12, Dec. 1975, pp. 988-1006.

3. Vittoria, C. and Wilsey, N.D., "Magnetostatic Wave Propagation Losses in an Anisotropic Insulating Medium," J.A.P., Vol. 45, p. 414, Jan. 1974.

4. Wu, H.J., Smith, C.V., Collins, J.H., Owens, J.M., "Bandpass Filtering with Multibar Magnetostatic - Surface-Wave Microstrip Transducers," Electronics Letters, 29 Sept. 1977, Vol. 13, No. 20, pp. 610, 611.

5. Ralston, A. and Wilf, M.S., Mathematical Methods for Digital Computers, Vol. I and II, Wiley (1967).

6. SYSTEM/360 Scientific Subroutine Package, Version III, Programmer's Manual, pp. 217, 218.

III. ANALYSIS OF PROPAGATION THROUGH MULTIPLE LAYERS OF METALLIC GRIDS (PROGRAM ALT)

Program ALT has been written to analyze the diffraction of an incident, lineary polarized plane wave at arbitrary incident angle by one or several metal strip grids.

Each strip has zero thickness, and width α_g (for the g-th grid). The grids each have the same spacing d_x and are located at positions Z_g. Each strip is infinitely long, and there are an infinite number of strips in each grid.

The incident wave has an arbitrary angle of incidence along the radial vector in conventional polar co-ordinates (r, θ, φ), with θ measured from the z-axis and φ measured from the x-axis of a rectangular co-ordinate system. The incident wave has its E-field polarized along the plane formed by $\hat{z}$ and the angle of incidence. Both components of scattered field are included. The parameters u and v are the direction cosines. These are inputed to the program as u and v. Q_M is the number of layers. The analysis assumes an indirectional current along the $\hat{Y}$ direction in each strip and solves for the complete diffraction field including primary and cross-polarized field and the radiation into grating lobes.

1. Computational Techniques and Numerical Analysis

The purpose of program ALT is to compute and print out the five components of the total field along with the values 20 logio of their magnitude.

These components allow the analysis of the propagation effects through a filter consisting of thin metal strips spaced d_x apart, with their axis oriented along the same direction.

The input parameters:

$$Q_M,\ \{a_m\},\ \{z_m\},\ d_x,\ u,\ v,\ PM\ (m = 1, 2, .., Q_M)$$

The output (components of the total field):

$T_s(P)$, $\Gamma(P)$, $T(P)$, $C+(P)$, $C-(P)$

$T_{sdB}(P)$, $\Gamma_{dB}(P)$, $T_{dB}(P)$, $C_{+\,dB}(P)$, $C_{-dB}(P)$

Y, CONTR (control sum for the checking of calculation).

These components are to be printed for each value of P, subject to the condition described below.

The complete solution breaks up into four parts:

1. Finding the elements of the vector $\{e\}$ where $e_m = -a_m e^{-jk_z z_m}$

$$k_z = 2\pi\sqrt{1 - u^2 - v^2}$$

2. Finding the elements (complex) of the matrix [c]

where

$$c_{mn} = \frac{(v^2-1)}{2d_x} \sum_{p=-\infty}^{\infty} e^{-jkp(|z_n - z_m|)} \left[\frac{2}{\beta_p} \sin\left(\frac{\beta_p a_n}{2}\right)\right] a_m \frac{\sin\left(\frac{\pi p a_m}{d_x}\right)}{\left(\frac{\pi p a_m}{d_x}\right)}$$

$$\frac{\sin\left(\frac{\pi p a_m}{d_x}\right)}{\frac{\pi p a_m}{d_x}} = 1 \qquad p \to 0 \quad ,$$

$$\frac{2 \sin\left(\frac{\beta_p a_n}{2}\right)}{\beta_p} = a_n \quad \beta_p \to 0 \quad ,$$

$$\beta_p = 2\pi\left(u + \frac{p}{d_x}\right); \qquad k_o = 2\pi; k_y = 2\pi v$$

$$k_p = \sqrt{k_o^2 - \beta_p^2 - k_y^2} \qquad \text{for} \qquad k_o^2 > \beta_p^2 + k_y^2$$

$$\sqrt{\beta_p^2 + k_y^2 - k_o^2} \qquad \text{for} \qquad k_o^2 < \beta_p^2 + k_y^2 \quad .$$

3. Solve the Matrix Equation:

$$[c] \{c\} = \{j\}$$

4. For each p, subject to the condition:

$$\beta_p^2 + k_y^2 < k_o^2$$

compute:

$$T_s(P) = F_+(P)\, k_o\, k_p \qquad Y = \frac{1 - \Gamma(0)}{1 + \Gamma(0)}$$

$$\Gamma(P) = F_-(P)\, k_o\, k_p$$

$$T(P) = \delta(P) + T_s(P)$$

$$C+(P) = -F_+(P)\, \beta_p\, k_y$$

$$C-(P) = -F_-(P)\, \beta_p\, k_y$$

along with 20 times the logarithm of their magnitude, where

$$\delta(P) = 1 \qquad \text{for} \qquad p = 0$$

$$F_+(P) = \frac{1}{-2(k_o^2 - \beta_p^2)\, k_o\, d_x} \sum_q jq\, \frac{e^{-jk_p z_q}}{} \sin\left(\frac{\beta_p a_q}{2}\right)$$

$$F_-(P) = \frac{1}{-2(k_o^2 - \beta_p^2)\, k_o\, d_x} \sum_q jq\, \frac{e^{jk_p z_q}}{\beta_p} \sin\left(\frac{\beta_p a_q}{2}\right) .$$

The control sum of the solution is:

$$P = \sum_p [\,|T(P)|^2 + |\Gamma(P)|\, C_+(P)|^2 + |C_-(P)|^2)]\, \frac{k_p}{k_o} ,$$

and should be equal to unity.

Because the elements of the matrix [c] are an infinite series of complex terms, the left and right bound of the sum-PM are chosen from 1 to 20, depending on the value of input parameters. (This series converges very rapidly). In the process of the solution of the matrix equation, the subroutine MINV[2], modified for complex elements, was used.

2. The Input and Output of Program ALT

The input to program ALT is contained in namelist INP. The parameters of namelist INP are:

QM - size of the matrix [c]

A(I) - value of the I-th element of the vector $\{a_m\}$

Z(I) - value of the I-th element of the vector $\{z_m\}$

DX - value of the d_x

V - value of the v

U - value of the u

PM - value of the left and right bounds of the sum (for the calculation elements of the matrix [c]).

The output of program ALT is printed. The printed output is:

1) The namelist INP (described in input).

2) The namelist OUT. The parameters of namelist OUT are:

P - value of p subject to the conditions described in FUNCTIONAL DESCRIPTION.

T - T(P) - value

TS - $T_s(P)$ - value

GAM - $\Gamma(P)$ - value

CPLUS - $C_+(P)$ - value

CMIN - $C_-(P)$ - value

TSDB - T_{sdB} - value

TDB - T_{dB} - value

GAMDB - Γ_{dB} - value

CPLUSD - C_{+dB} - value

CMINDB - C_{-dB} - value

Y - Y_- value

CONTR - P- value

If any of the values don't exist, the corresponding message is printed.

The value of CONTR (on output) should be equal to unity. If CONTR is not equal to unity, it means that input data (parameters) don't satisfy the restrictions 1-4.

3. REFERENCES

1. Larsen, T., A Survey of the Theory of Wire Grids, IRE Transactions on Microwave Theory and Techniques, May 1962, pp. 191-201.

2. System/360 Scientific Subroutine Package, Version III, Programmer's Manual, pp. 118.

IV. DETECTION OF SIGNALS IN NOISE AND CLUTTER

1. Introduction

The request was made, to numerically evaluate some multiple integrals having to do with the detection of radar signals in the presence of background noise and ground clutter. In particular, the integrals P_{d1} and P_{d2}, given below, are probabilities that a radar detection system identifies an existing target, such as a missile or airplane, while set at a particular threshold level and receiving N reflected pulses per sweep. The integral P_f is the probability that a "false alarm" occurs: that a "target" be seen when none is actually present.

The difference between P_{d1} and P_{d2} is that in the latter case, any fluctuations in the target are assumed to occur slowly in comparison to the repetition rate of the pulses within each sweep, whereas in the former, the fluctuations may be rapid. Thus, for the special case N = 1, the triple integral P_{d1} must reduce to the double integral P_{d2}. This was checked analytically. Moreover, for the special case in which there is no signal (signal to noise ratio zero), P_d reduces to P_f regardless of N. The assumptions are made that the signal and the noise are Rayleigh-distributed, and that the clutter has a long-normal distribution.

The integrals, transformed to the most convenient form for computation, are

$$P_{d1} = 1 - \frac{1}{2\sqrt{2\pi}\sigma} \int_o^{y_o} e^{-y}\, dy \int_o^{\infty} d\xi\, e^{-(1+N\alpha)\xi} G_N(y, N\alpha\xi) \int_o^{\infty} ds\, \frac{1}{s} e^{-s} I_o(2\sqrt{\xi s}) \times \exp\left\{ -\frac{1}{8\sigma^2} \ln^2(2\alpha\beta s) \right\}$$

$$P_{d2} = 1 - \frac{1}{2\sqrt{2\pi}\sigma} \int_o^{\frac{y_o}{1+\alpha}} e^{-y}\, dy \int_o^{\infty} ds\, \frac{1}{s} e^{-s}\, G_N(y, s) \exp\left\{ -\frac{1}{8\sigma^2} \ln^2\left(\frac{2\beta(1+\alpha)s}{N}\right) \right\}$$

P_f is identical to P_{d2} when the parameter α is taken to be zero. The $G_N(y, s)$ are

$$G_N(y, s) = \sqrt{\frac{y}{s}}^{N-1} I_{N-1}(2\sqrt{ys})$$

$I_N(x)$ is the Modified Bessel Function of order N and argument x,

N = number of pulses per sweep,

α = signal to noise ratio,

β = noise to clutter ratio,

σ = variance of the log-normal clutter distribution,

y_o = threshold level setting

The objective (for each desired N, β and σ) was to calculate P_f as a function of y_o, thereby establishing values of y_o for which P_f was satisfactorily small; and then, using these y_o, to find P_{d1} and P_{d2} as a function of α, proceeding from small α to values large enough that the probability of detection reaches at least .99.

2. Results

The parameters used are listed below:

$N = 1, 3, 6, 10$

$\beta = \sqrt{.1}, 1, \sqrt{10}, 10, 100$

$\sigma = 0.7, 1.1, 1.6$

$P_f = 10^{-4}, 10^{-6}$

The values of y_o required to give sufficiently small P_f have the following dependence on the parameters: the larger β is, the smaller y_o; the larger N is, the larger y_o; and the larger σ is, the larger y_o. The dependence on N and β is strong, but the dependence on σ is even more so. In fact, values of y_o for $\sigma = 1.1$ and 1.6 were so large that the computer time required to do the integrals was considerable, and these cases were dropped after a cursory investigation.

Table 1 gives the values determined for y_o for different cases.

By making the assumption that $y_o >> 1$, one can show that

$$P_f = \frac{1}{2} \operatorname{erfc}\left[\frac{1}{\sqrt{2}\sigma} \ln\left(\frac{2\beta y_o}{N}\right)\right]$$

where erfc(x) is the complementary error function. This expression is quite accurate for $\beta \leq \sqrt{10}$, and serves as a check on the numerical results. As β increases above 5, the approximate expression becomes progressively less accurate.

P_{d2} was then calculated as a function of α. The function rises sharply (from P_f) as α increases from zero, then flattens out and slowly approaches 1 as α becomes large. This is illustrated in Figure 1 for a typical case. The larger β is, the larger P_{d2} is for a given α. (Equivalently, for larger β, smaller α are required to get a fixed detection probability.) In the flat part of the curve, larger N give larger values of P_{d2}.

It was possible to derive a limiting expression for P_{d2} which is valid in the limit of large α:

$$P_{d2} \simeq \exp\left(-\frac{y_o}{1+\alpha}\right) \sum_{m=0}^{N-1} \left(\frac{y_o}{1+\alpha}\right)^m \frac{1}{m!}$$

This provides a quick and accurate answer for $\alpha > y_o$ and also serves as a check on the numerical results for such cases.

Tables 2 and 3 give the values of α for which P_{d2} is equal to .9, .99, and .999, when $P_f = 10^{-4}$ and $P_f = 10^{-6}$, respectively.

P_{d1} was also calculated for different α. For N = 1, the results should be, and are, identical to P_{d2}. For N > 1, the function behaves much the way P_{d2} does when β is varied. However, a variation of N has very little effect: the results are similar for all N.

A limiting expression was derived for P_{d1} for large α:

$$P_{d1} \simeq \left[1 - \left(1 + \frac{1}{N\alpha}\right)^{N-1}\right] + \left(1 + \frac{1}{N\alpha}\right)^{N-1} \exp\left(-\frac{y_o}{1+N\alpha}\right) \simeq \exp\left(-\frac{y_o}{1+N\alpha}\right)$$

It is possible to do the ξ- and y- integrals in P_{d1} analytically. The result is an infinite series, with Gauss hypergeometric functions[1] in the integrand of the s-integral in each term. The convergence properties of the series are unknown, and this approach was not pursued vigorously.

3. Programs

P_f and P_{d2} are calculated in program PPWNO8, and P_{d1} is calculated in PPW12. The input data for each program are read from a single card for each run. These are described in detail in the program listings.

4. PPWNO8

The repeated computation of the s- integral is the most time-consuming portion of the job. The front edge of the s- integral ($0 \leq s \leq 1$, where the integrand varies most rapidly) is done with an adaptive Simpson's rule routine.[2] This uses an interval-halving procedure which minimizes the number of integrand evaluations. The rest of the s- integral, $1 \leq s \leq s_{max}$, is done by m-point Gauss-Legendre quadrature,[3] where m is read in. The region 1 to s_{max} is divided into pieces (up to 8 of them) whose width depends on y. The integration proceeds piece to piece in the direction of increasing s until one piece gives a negligible contribution to the total. If the 8th interval still contributes, a 9th interval (s_{max} to ∞) is processed by making the transformation $x = 1/s$ and integrating $0 \leq x \leq 1/s_{max}$. Otherwise, s_{max} is a substitute for ∞.

When y is small, the s- integrand drops off slowly as s increases beyond y. For large y, it is sharply peaked at $s \simeq y$. In many such cases the region $0 \leq s \leq 1$ contributes negligibly, so the worst part of the computation can be avoided.

The y- integration is done by m'-point Gaussian quadrature, m' being read in. For N = 1, the integrand decreases monotonically from y = 0; for N>1, it peaks at small y. In the latter case, two intervals are integrated separately, for improved accuracy.

The main program reads in the input data, prints it, and calculates the limiting case (for large α, to compare with P_{d2}). Subroutine CHOICE chooses the desired m'-point Gaussian quadrature subroutine DQGm.[4] Function FN is the y- integrand. It calls CHOIC, which selects DQGm, which integrates function SINT, the s-integrand.

5. PPW12

The triple integral P_{d1} was transformed so that the s- integral would look exactly like that of P_{d2}, except that $I_o(2\sqrt{\xi s})$ is substituted for $G_N(y, \xi)$. The same comments about the shape of the s- integrand apply. The region $0 \leq s \leq \infty$ is divided into pieces exactly as before, but an adaptive 4-point Gaussian integration subroutine AQG4 was written to replace the adaptive Simpson's (ASQ) and standard Gaussian routines. The superior accuracy of the Gauss-Legendre formula offsets the inherent efficiency (not recomputing any integrands) of ASQ and provides a somewhat (up to 20%) faster evaluation of the s- integral, for a given required accuracy.

The ξ- integrand, typically, is very sharply peaked at $\xi = y/N\alpha$. AQG4 is used for this integral also, as it is for the y- integral, which is much like the y- integral in P_{d2}.

The s- integral, being the most deeply imbedded, is required so frequently that it is efficient to compute a table consisting of ξ and the s- integral, and interpolate whenever a value of the latter is needed. This saves a great deal of time.

The main program reads the input data, prints it, and calculates the interpolation table by calling SINTGL. This subroutine performs the s- integral by calling AQG4 to integrate function SINT. The main program then calculates a divided difference table from the interpolation table, to estimate the worst errors likely to be made by the Aitken-Lagrange interpolation[5] procedure using INT table entries. INT is automatically adjusted upwards (to a limit of 9) if greater accuracy is required. It then does the remaining integrations by calling AQG4W, which integrates function YINT, the y- integrand. YINT

sets the limits for the ξ- integration and calls AQG4P to perform it. Function CSINT calculates the ξ- integrand. Part of the latter procedure consists of calling subroutine INTERP, which orders the table entries, and ALI,[6] which performs the interpolation itself.

Creating the table requires the most time, so it is advantageous to use it for more than one case at a time. If the product $\beta \cdot \alpha$ remains unchanged from one case to the next, the table is not recomputed. The required range for the table ($0 \leq \xi \leq$ CSIMAX) is slightly greater for smaller N for a given $\beta \cdot \alpha$, so a case with N = 1 should be followed rather than preceded by cases with N > 1. If this is not done and a point outside the table range is required, CSINT calls SINTGL to calculate it rather than extrapolating from the table.

6. IN and INASYM

These subroutines were written to calculate the modified Bessel functions $I_n(x)$ to any desired accuracy. IN uses the infinite series representation[7] which converges rapidly for small x, while INASYM uses an asymptotic series[7] and is useful for large x. Tests show that for a desired accuracy of 10^{-k}, IN is more efficient for $x < k + n$ and INASYM should be used otherwise. For n = 0 or 1, the cutoff point is $x < k + 2$.

N	L	$\beta = \sqrt{.1}$	1	$\sqrt{10}$	10	100	$\sqrt{10}$	$\sqrt{10}$
1	4	287	94.96	30	13.67	9.35	565	23,265
3	4	835	279.41	90	33.46	14.23	1680	
6	4	1735	556.11	180	63.68	20.19	3400	
10	4	2900	925.07	300	104.15	27.41	5640	
1	5	630	200	66	23		1875	
3	5	1880	598	192	62		5650	
6	5	3720	1180	400	129		11294	
10	5	6220	1970	630	208		18781	
1	6	1240	390	125	43.44	14.11	5600	
3	6	3700	1170	375	122.96	20.76	16500	
6	6	7400	2350	730	242.42	33.67	32850	
10	6	12400	3880	1240	402.70	53.00	55860	
1	7	2300	700	235	77			
3	7	6800	2170	700	223			
6	7		4350	1400	440			
10	7		7250	2250	765			

Table 1. Values of y_o, determined from program PPWNO8, for which $P_f = 10^{-L}$. $\sigma = 0.7$ except for the sixth column, where $\sigma = 1.1$, and the last, where $\sigma = 1.6$. Values without decimals are accurate to 5%; others are accurate to the last decimal given.

N	P_{d2}	$\beta = \sqrt{.1}$	1	$\sqrt{10}$	10	100
1	.9	2723	872	284	129	87.8
1	.99	2.86×10^4	9150	2985	1360	930
1	.999	2.87×10^5	9.20×10^4	3.00×10^4	1.37×10^4	9348
3	.9	750	250	80	29.5	11.8
3	.99	1900	630	205	76.0	31.7
3	.999	4350	1430	470	175	74.0
6	.9	547	175	56.0	19.2	5.47
6	.99	965	227	99.6	34	10.3
6	.999	1560	320	169.6	56	17.0
10	.9	466	151	47	15.7	3.4
10	.99	693	228	71.6	24	5.6
10	.999	963	320	100	34	8.2

Table 2. Values of α, determined from program PPWNO8, for which $P_{d2} = .9, .99,$ and $.999$. $\sigma = 0.7$ and $P_f = 10^{-4}$.

N	P_{d2}	$\beta = \sqrt{.1}$	1	$\sqrt{10}$	10	100
1	.9	$1.18 \times 10^{4}_{5}$	$3.70 \times 10^{3}_{4}$	$1.19 \times 10^{3}_{4}$	411	133
1	.99	$1.23 \times 10^{5}_{6}$	$3.88 \times 10^{4}_{5}$	$1.24 \times 10^{4}_{5}$	4321	1403
1	.999	1.24×10^{6}	3.90×10^{5}	1.24×10^{5}	4.34×10^{4}	1.41×10^{4}
3	.9	3380	1055	348	113	17.7
3	.99	8500	2680	855	280	46
3	.999	1.93×10^{4}	6100	1950	640	107
6	.9	2350	640	234	75.5	9.7
6	.99	4150	1300	412	135	17.8
6	.999	6650	2120	660	240	29.5
10	.9	1980	620	197	64	7.6
10	.99	3000	937	298	96	11.8
10	.999	4350	1300	415	137	16.9

Table 3. Values of α, determined from program PPWNO8, for which $P_{d2} = .9, .99,$ and $.999$. $\sigma = 0.7$ and $P_f = 10^{-6}$.

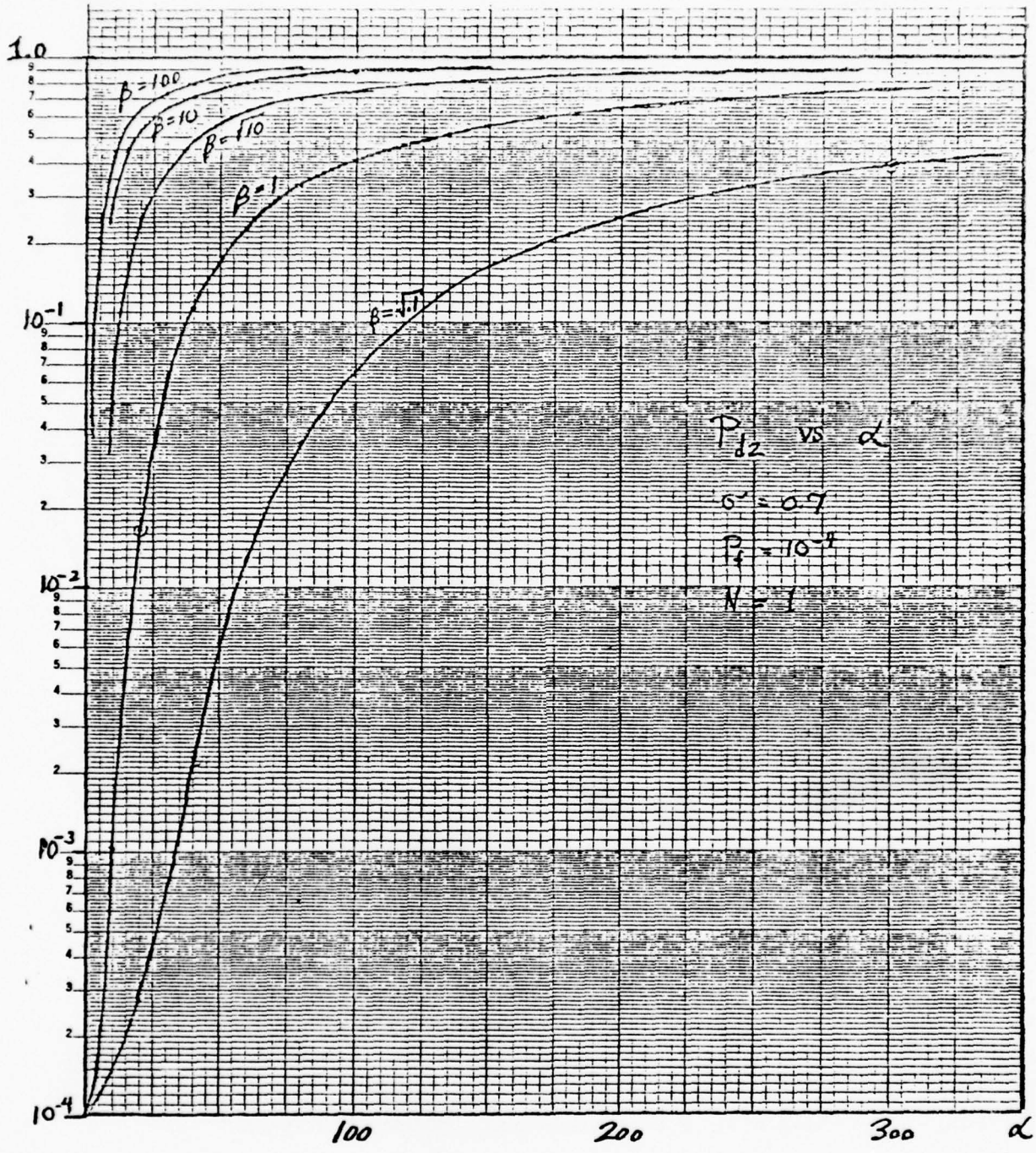

Figure 1. P_{d2} vs. α for N = 1 and different values of β.

REFERENCES

1. M. Abramowitz and I. A. Stegun, eds, Handbook of Mathematical Functions, N. B. S. Applied Mathematics Series, Washington, U. S. Government Printing Office, 1964, p. 556.

2. L. F. Shampine and R. C. Allen, Numerical Computing: An Introduction, Philadelphia, Saunders, 1973.

3. P. J. Davis and P. Rabinowitz, Numerical Integration, Waltham, Blaisdell, 1967.

4. System/360 Scientific Subroutine Package Version III, White Plains, IBM Tech. Pubs. Dept., 1968, p. 299.

5. F. B. Hildebrand, Introduction to Numerical Analysis, N. Y., McGraw-Hill, 1956.

6. Ref. 4, p. 242.

7. Ref. 1, p. 374 ff.

V. MAPPING PROGRAM

1. Introduction

The request was made, to modify and supplement certain subroutines provided by the initiator, write some new ones, and then combine them so that all the results would be available simultaneously. The objective was to produce a computer-drawn map of the earth, or certain portions of the earth, with any desired great circle, or any other arc or line, superposed on it, and with certain labels in the appropriate places.

The complete program consists of a main program, MAP, two sets of subroutines, and a block data program. The subroutines DEC, CONV, and POINTS, and block data DIPEQ, are used for producing sets of points (latitude, longitude) to be plotted on the map. The subroutines SUPMAP, MAPLOT, SUPCON, and FRSTPT are used to read these data, transform the (lat, lon) coordinates to a form (u, v) suitable for the desired projection, and do the actual plotting. (For pen plotting, subroutine CODE also prints the map parameters next to the map.) The standard CRT or PEN routines are required, as well.

2. Description of the Program

2.1 General

In their original form, SUPMAP, MAPLOT, SUPCON and FRSTPT are capable of producing the map itself, which shows the land contours with a resolution of about .1°. The use of these subroutines, and the options available are described in the mimeographed pamphlet "World Map Plot." The mapping function remains substantially unchanged, and will not be discussed here. A data file containing the latitude and longitude of the necessary points was provided, and presently exists as a permanent file (WMAP DATAX2401, CY=2, ID=WINTERS). This must be attached as TAPE4, and is read with an unformatted read in MAPLOT.

The main program, MAP, has six sections. These are an initialization section, four optional sections which generate points for lines to be drawn on the map, and a final part which calls the mapping subroutines to do the actual drawing. The four optional sections are controlled by the integer parameters NOGC, DIP, AUR, and NOLN, which are read at statement 250 (along with parameter CRT). A value of zero for any of these, causes that section to be skipped. A negative value permits—and a positive value suppresses—the printing of the points which are generated. A considerable amount of information is provided in the comment section of the program listing. In particular, there is a description of the use of each input parameter. In some cases, the result of selecting each of the possible acceptable values for the parameter is also given in detail. These comments are found just before or just after the corresponding read statements. The user should refer to them for detailed information.

2.2 Great Circles

NOGC is the number of great circles to be calculated and drawn. The user supplies the latitude and longitude of the end points of the great circle, and the program produces a locus of points along it. Optionally, the program can be told to use the latitude and longitude coordinates of any of eight preassigned locations as one end point, in which case the user supplies only the other end point. (The eight fixed locations are the VLF broadcast stations of the worldwide Omega navigation system.) One, several, or all eight stations can be automatically used as one end point, with a single user-supplied point for the other.

This section requires some input data. The necessary parameters are read at statement 100, and the end points are read in between statements 120 and 160. A detailed explanation is given in the program listing.

On a spherical earth, a great-circle between points A (θ_o, Φ_o) and B $(\theta_1 \Phi_1)$ has an arc length, in radians, of

$$\psi = \arccos \left\{ \sin\theta_o \sin\theta_1 + \cos\theta_o \cos\theta_1 \cos\Delta\Phi \right\} \qquad 1)$$

where $\Delta\Phi$ is the difference in the longitude coordinates and θ represents latitude. Then the locus of points (θ, Φ) on the great circle is given by

$$\Phi - \Phi_o = \text{arc sin} \left\{ \tan\alpha \tan\theta_o \right\} - \text{arc sin} \left\{ \tan\alpha \tan\theta \right\} \qquad 2)$$

where α gives the arc length between the north pole and that point on the great circle nearest the pole:

$$\alpha = \arcsin \left\{ \frac{\cos\theta_o \cos\theta_1 \sin\Delta\Phi}{\sin\psi} \right\} \quad . \qquad 3)$$

Subroutine DEC is used to calculate the arc-length ψ. Then, using ψ, subroutine POINTS finds the locus of points, which is the desired output. Subroutine CONV is used, at the beginning, to convert the end-point coordinates, which are read as pairs of seven-digit floating point numbers DDDMMSS representing degrees, minutes, and seconds, to radians and decimal degrees.

2.3 Dip Equator

Any nonzero value for DIP indicates that the magnetic dip equator should be drawn. The latitude points are stored in block data DIPEQ and

in COMMON/C/ and correspond to longitude intervals of 5° starting at -180°. No data cards are required for this section.

2.4 Auroral Oval

Any nonzero value of AUR indicates that the northern auroral oval should be drawn. All comments pertaining to the dip equator are valid for this section as well.

2.5 Lines to be Read In

NOLN is the total number of points to be read in, if other lines or contours are to be drawn on the map. The coordinates can be read in -one pair per card- as seven-digit numbers DDDMMSS representing degrees, minutes and seconds, or as decimal degrees. In the former case, subroutine CONV converts them to decimal degrees. Details are in the program listing.

If more than one distinct line is to be read in, the last card of each line must contain an impossible coordinate, such as latitude = 100. This "break point" tells the plotter to lift the pen when going from one line to the next. These points are counted as part of NOLN. If one wishes to avoid counting points to find NOLN, one can terminate this section by setting NOLN equal to a very large number and doing one of two things:
a) read in two consecutive cards with impossible latitude coordinates, or
b) read in a card with 'X' punched in column 1.

2.6 Storing the Points

The points generated in the optional sections are all found before any plotting begins. Initially, they are stored in a 250x2 array STORE. Break points are inserted automatically after each line generated. When the

array is full, the numbers are written to a scratch file, TAPE8, along with the number, NUM, of pairs. The array then is filled again, and so on. At the end, however many points remain in STORE are written to TAPE8. After the map is complete, TAPE8 is read, 250 pairs at a time and the lines are drawn by a procedure which is identical to that for the map itself.

2.7 Miscellaneous Comments

This program has been run on the AFGL CDC-6600 computer using the operating system SCOPE 3.4.4 and the FTN compiler. The memory requirement is about 62000 octal words, slightly above the system default. The compilation time is about 7 seconds and a single map requires between 10 and 15 seconds beyond this. Virtually all of this time is used for the map itself; very little is used for the great-circle calculations.

The program will do several maps consecutively. A full set of data cards must be read in for each map. After each one, the program returns to statement 1 and begins reading again. A blank card or end-of-file at that point terminates program execution.

Parameter CRT, an integer read at statement 250, should be zero for PEN plots and nonzero for CRT plots.

Whenever (latitude, longitude) pairs are read in, a field of 20 spaces of alphanumeric information beginning in column 22 is also read. This purely optional feature allows one to identify any location by name, and have the name printed on the output listing (not the map).

3. Examples

3.1 Use of the Program

The following deck can be used to produce a map with the on-line plotter

```
WIN53,CM65000.                          3435 WINTERSTEINER
REQUEST (PLOT,*Q)
ATTACH (XX,.....                                    file containing source
FTN (I=XX,SL,R=3)                                           program
ATTACH (PEN,ONLINEPEN)
ATTACH (TAPE4, WMAPDATAX2401,ID=WINTERS,CY=2)       file containing map
LIBRARY (PEN)                                                 data
LGO.
DISPOSE (PLOT,*OL)
7/8/9
data
6/7/8/9
```

The following list contains the input parameters and the format in which they are to be used. The data listed are sufficient to produce a view of the earth from above the North Atlantic. The northern auroral oval is drawn, as is a great circle from Boston to Vienna, and another line (read in) connecting these cities. Great circles from Bermuda to omega stations B, D, F, and G are drawn, even though F will be off the map. The map will be 8" X 8", drawn with pen and ink with grid spacings every 10°. The coordinates of the great circles, and those of the line read in, will be printed. Those of the auroral oval will be suppressed.

```
JPROJ,ITYPE,JGRID,ISWAP                          4i5      2    1   10    0
CLAT,CLON,ROT                                  3f10.4   45.0000  -40.0000   0.0000
ULEN,VLEN                                      2f10.4    8.0000    8.0000

NOGC,DIP,AUR,NOLN,CRT                            5i5     -5    0    1 -600    0

OMEGA,CNTR,READ,NOPTS,(ILL(I),I=1,6)
                                        4i5,6(4x,a1)     0    1    0   50
ALAT,ALON,M1,M2                        2f10.0,1x,2a10   422000   -710500   BOSTON
BLAT,BLON,N1,N2                        2f10.0,1x,2a10   481300    162200   VIENNA

OMEGA,.....                                              1    9    0   50   C   E   H   A
ALAT,....                                               320000   -650000   BERMUDA

ALAT,ALON,M1,M2          a1,f9.0,f10.0,1x,2a10          42.333   -71.083   BOSTON
ALAT,ALON,M1,M2          a1,f9.0,f10.0,1x,2a10          42.468   -69.083
  .                                                       .
  .                                                       .
  .                                                       .
ALAT,ALON,M1,M2          a1,f9.0,f10.0,1x,2a10          48.119    16.367 VIENNA
ALAT,ALON,M1,M2          a1,f9.0,f10.0,1x,2a10 X
```

The first three cards are the map parameters (see mimeographed pamphlet). The fourth gives the program options (see Section II). The next three give the parameters and end points for the first great circle, and the following two are for the remaining four great circles (see program listing). The last set of cards contains the coordinates, in decimal degrees, of a single desired line.

3.2 Examples

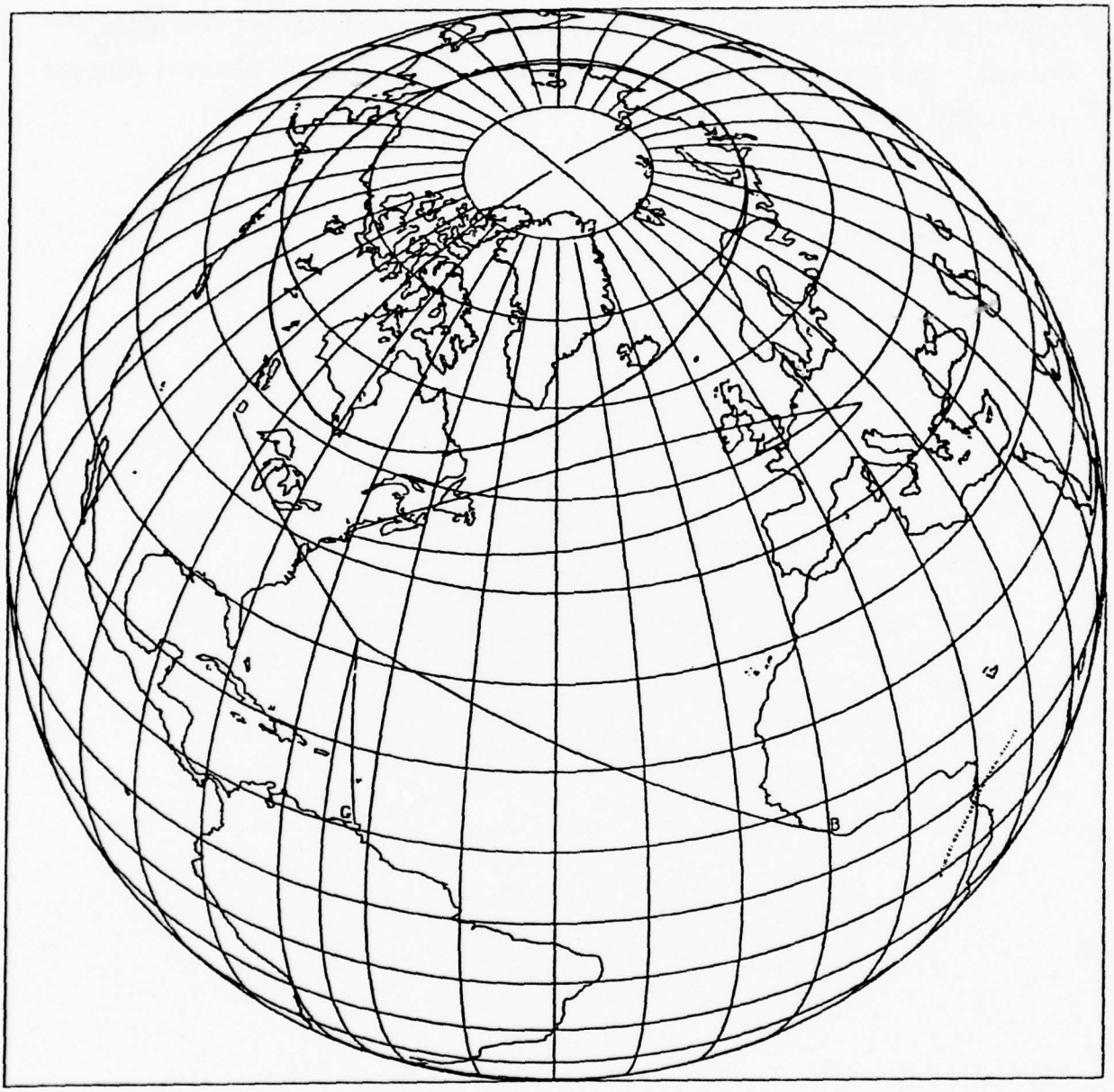

Orthographic projection, described in section III. 1

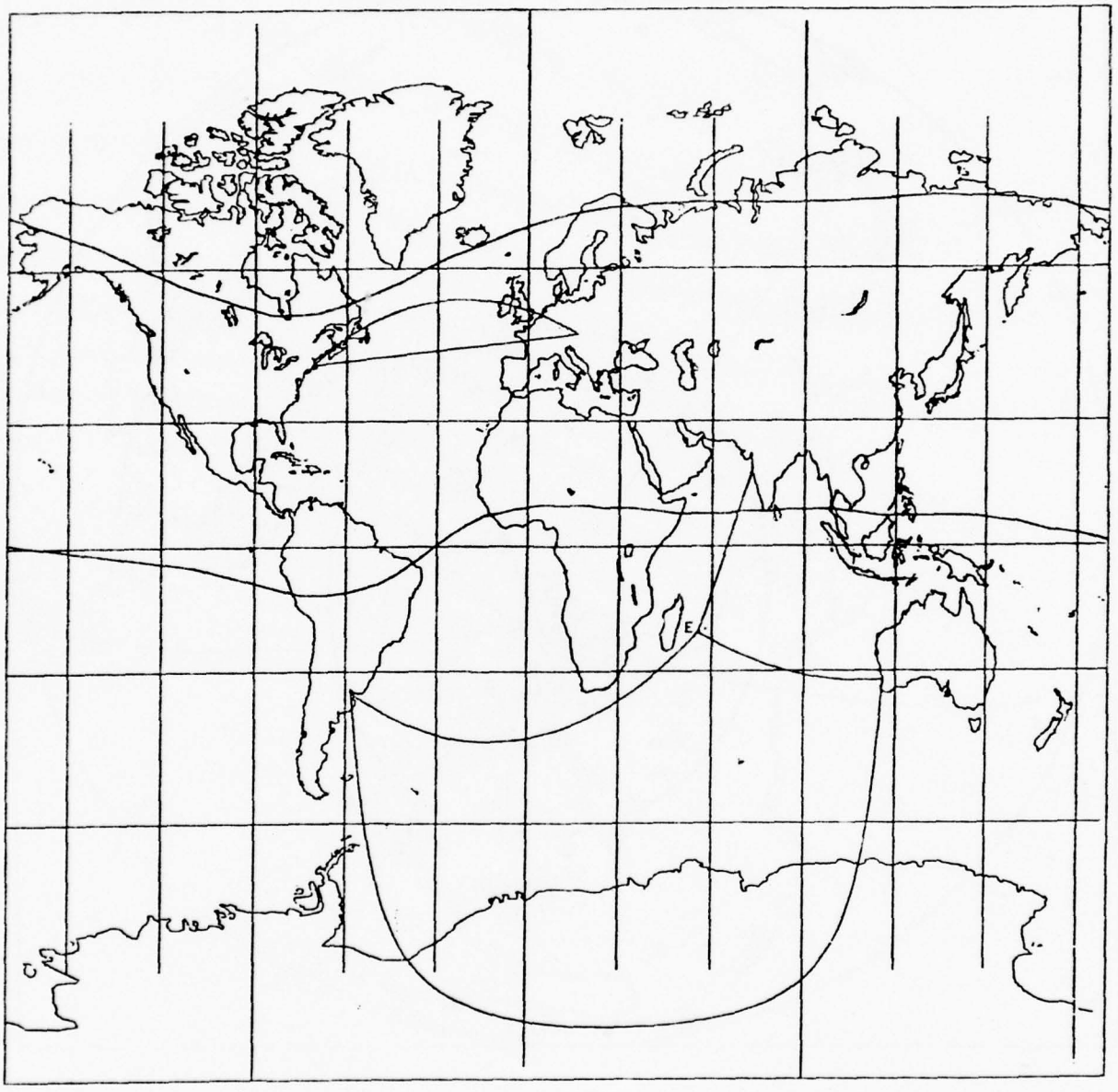

Miller Modified Mercator projection with magnetic equator, auroral oval, great circles and one line read in.

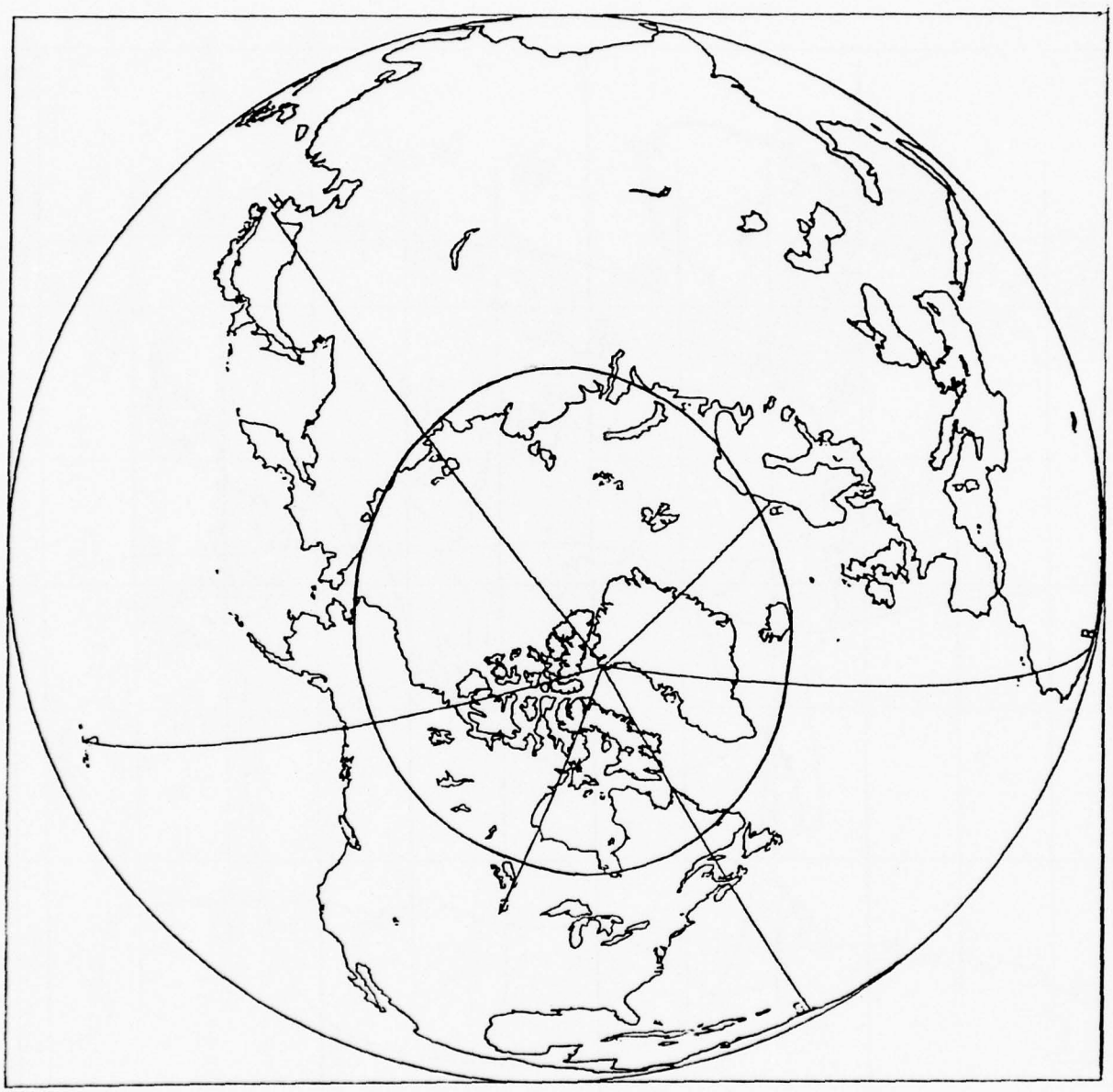

Orthographic projection, view from above North Pole
with auroral oval and great circles.

VI. PROGRAMS FOR PROCESSING POLAR VLF PROPAGATION DATA

1. Introduction

The Propagation Branch of the Electromagnetic Sciences Division, R. A. D. C., is engaged in ongoing research involving continuous measurements of many ionospheric and atmospheric parameters. Analog data from their various instruments are fed to a data acquisition system which digitizes them and writes them onto tape for storage and subsequent retrieval. With the introduction of a new acquisition system it became necessary to revise the data-handling procedures. Two programs were requested and developed to satisfy the requirements.

The objective of the first program is to read the BCD-coded field tapes as quickly as possible, check for errors, and write all the useful raw data, packed as efficiently as possible, onto a backup tape in the original sequence. The objective of the second is to read the backup tape, convert the raw data to physical units, sort it efficiently, and plot it channel by channel. The methods by which this is done, and the subsidiary functions of the two programs, are outlined below.

The field tapes contain information from many different sensors ("channels"). A single scan of all the channels is identified by an "experiment time." The field tapes consist of a sequence of such scans, each of which includes some recognition characters, the experiment time, some "fixed data" which remains the same from scan to scan, and the raw experiment data. To provide some organization to this stream of data, a certain number of scans are grouped into single records, which can be up to 4096 characters in length.

In the present arrangement, 40 channels are scanned and 15 scans constitute a record. The scans are 265 characters in length; the records, 3975. It is possible to prepare field tapes in other formats, and the programs accommodate them with minimal changes.

There is no requirement that the scans be equally spaced in time, but the normal circumstance is one scan every 30 seconds, or one record every 7-1/2 minutes. At this rate, a continuous run of 60 days' duration would produce 6,912,000 separate data points, or 172,800 points per channel, in 11520 records.

The need to examine such large amounts of information is the reason for the plots. Two plot options are offered: 1) an average over a certain time interval, known as an "averaging period," and 2) the scan-by-scan results. Even in the latter case, time is organized into averaging periods for convenience.

2. Program BACKUP

A) Reading the Field Tape

Complete records of good field data consist of 15 identical scans, in the present arrangement. The BCD code for each of the 265 characters in a scan occupies 2 octal digits, or 6 bits. When a record is read into central memory, 10 characters fit into each 60 bit word, but there is no particular correlation between words and meaningful groups of characters (such as single data-values). Appendix B illustrates this point.

The assumed format for each scan is

"CLDDD<HH<MM<SSCL TTTYYJ±NNNNN±NNNNN.....±NNNNN

", C, L, <, and (space) represent the BCD codes for those characters. DDD represents the BCD code for three digits giving the day of the year, while HH, MM, and SS stand for the hour, minute, and second of the scan in question. TTT, YY, and J stand for the codes for digits representing

the time interval (in seconds) between consecutive scans, the year (e.g. 78) and the system code (1 or 2). (Together these three constitute the "fixed data.")

The first field ±NNNNN stands for a positive or negative 5-digit integer giving the data in the first channel, and there are 40 such fields per scan.

The strategy of BACKUP is to buffer a complete record into array A, and interpret it with one DECODE statement. The DECODE operation translates the code to numbers and stores them in 15-element arrays. For example, DDD is decoded into an integer, ddd, and placed in array T(NS, 1) according to format I3. (NS identifies the scan, 1 to 15) hh, mm, and ss are also stored. The channel data are put into STORE(NS, N), where N ranges from 1 to 40. The special symbol "CL is stored in SPS(NS) and the other special characters are ignored.

Any records with parity errors are ignored, as are those containing an unexpected number of words.

B) Checking the Records

A variety of abnormal conditions can occur:

1) A time interval other than normal can appear between consecutive scans on the same record, or on different records.

2) A temporary shutdown after some scan will result in filling the remaining characters of the record with the BCD code for $.

3) An extra character or two can be inserted somewhere in an otherwise normal record.

4) The fixed data on the tape may not agree with the expected fixed data values which are read in.

Note that if 2) occurs, 1) is likely to occur also. Whenever 1) occurs, the program makes note of it and proceeds. If 2) occurs, the DECODE operation has failed since $ appears where a number should be. However, the program is prevented from terminating or printing diagnostics by previous calls to ERRSET and SYSTEMC. The same record is then decoded scan by scan until the first error is encountered again, and all the good scans are saved.

Occurrence of 3) causes the DECODE to fail also. Scans including and following the one with the first extra character will be lost.

Condition 4) can cause rejection of the record, or be ignored, at the user's option.

After the various checks are satisfied, all the scans of useful information are put onto the backup tape.

C) Packing the Backup Tape

For each field-tape record processed, one backup-tape record is written. Array B is used to store the information as it is processed.

Each backup record begins with a single 60-bit word containing the fixed data information and the BCD code for the special recognition symbol "'''''', which requires 24 bits (64646464 octal). The fixed data are represented as an integer tttyyj and use the other 36 bits. The integer 30781 indicates 30-second scan intervals, 1978, and system 1.

Each of the 15 scans requires 15 words, so the complete record is 226 words long. The first of these 15 words contains a recognition symbol, " (6 bits) followed by a single right-justified integer yydddhhmmss, such as 78010023000 giving the experiment time. The 2nd through 15th words are reserved for the channel data, 3 channels to a word. That is,

the first 20 bits of word 2 of any scan contain the integer corresponding to NNNNN from channel 1; the second 20 bits, from channel 2; and so on. The last 40 bits of the 15th word of each scan are zeros, and a new scan begins with a new word.

The recognition symbols are stored as BCD codes by routine MXPUTX, the integers as simple numbers by ISBYTX. The raw channel data range from -39999 to +39999 (millivolts). To avoid sign problems, the positive data are biased by +40000 and the negative data are stored as their absolute values.

A buffer out operation completes the processing of each record.

D) Use of the Program

1. Required Input Files

a) TAPE4: The field tape, which should have an L designation on the REQUEST card.

b) INPUT (TAPE5): One card-image containing the following information in format 9I5, I10. Typical values are given in parentheses.

NFX	= the number of files to be read from the field tape	(1)
NWX	= the number of words per record	(398)
NCH	= the number of channels per scan	(40)
NSCAN	= the number of scans per record	(15)
SCAN	= the expected time interval between scans (seconds)	(30)
YR	= the expected year in which the experiment began	(78)
IC	= the expected system code	(1 or 2)
NFLAG	= 0 or 1 (see below)	(0)
RMAX	= total number of records to be read	(0)
TMAX	= last experiment time to be processed (dddhhmmss)	(0)

SCAN, YR, and IC are to be compared with the fixed data of the first scan of each record. If NFLAG = 0, any inconsistencies will be noted but otherwise ignored. If NFLAG = 1, inconsistencies result in rejection of the record. If RMAX and TMAX are zero, the program reads to the end of the last file.

2. Memory and Time

The program requires about 41000 (octal) words of core. Execution time is approximately .1 sec for every good record processed. Frequent interruptions increase this somewhat.

3. Miscellaneous

The time on the backup tape is stored as a single integer yydddhhmmss. The program recognizes a change of year, going for example from 77365235959 to 78001000000 instead of to 77366000000. It also recognizes leap years.

3. Program READ

A) Basic Organization

The handling and plotting of data are controlled by a table of directives, DRCTV, which is read in and which contains 15 entries for each of the 40 channels which could be used. This is described in Section III-D and APPENDIX A.

Of all the data found on the backup tape, only some of it may be of interest. A "time window" giving the first and last experiment times desired is read in, and ---except for the time words---only scans in this range are read.

The sheer volume of information to be processed makes the use of a direct-access file attractive. Suppose there are 170,000 scans of 40

channels, to be read in the original time sequence. One first wishes to plot the information obtained over the entire time range for just one channel, and then information from the entire time range for the next channel, and so on. Even lumping 20 scans to an averaging period, core storage for some 340,000 points is lacking. Most alternatives to core storage involve rewinding and rereading one or more sequential files to pick out every 40th point (or even every 40th group of points) and are cumbersome and costly in time.

The WRITMS and READMS mass storage routines allow one to write many records to a scratch file and recover them in any desired order. The strategy of program READ is therefore to read the tape until a large, but not unmanageably large, number of points has been obtained. These are sorted according to channel, and when the array containing them (chosen to be 10240 points) is full, separate records are written containing information from each channel, using WRITMS on the random-access file TAPE8. The array is then refilled and the process repeats. If all 40 channels are used, the data from channel 1 appear on records 1, 41, 81,.... which can be recovered in order without reference to records 2-40, 42-80, etc. Data from channel 2 is on records 2, 42, 82, ... and so on.

Note that, while data from all 40 channels is on the backup tape, one can disregard as many of the 40 as one wishes after reading them. Note also that the "number of points obtained" depends on the plot option. If averaged data are plotted, there is only one point per channel per averaging period, regardless of the number of points used to get the average. If scan-by-scan results are plotted, all data points are "obtained."

The program logic is best understood as an organization of the sequence of experiment times found in the time window into different

blocks of time. A single scan occurs at an instant in time. Each averaging period contains whatever number of scans that fall within its boundaries. (Averaging periods start at the beginning of the time window and run consecutively to the end; if there are time gaps on the tape, some periods may have fewer scans than normal, or maybe no scans.) Each dump contains data from as many averaging periods as can be stored in 10240 words. As such, the time interval represented by a single dump depends on the number of channels being processed, and the plot option. (A dump is actually the process of writing records to TAPE8.)

No more than 1360 records can be dumped in all, so if there is more information than these can hold, a plot must be performed before the backup tape can be read any further. A plot period is whatever time interval it takes to fill 1360 records. In normal circumstances it is not necessary to go to a second plot period.

For sake of illustration, suppose that only 32 channels are to be plotted. Then each dump can contain 320 averaging periods, since 320x32 = 10240. If the averaging periods are 600 seconds in length, each dump will represent 192,000 seconds, or 2.22 days. At 32 records per dump, 42 dumps can be made before the allowable number of records is exceeded. A plot period is therefore 93.33 days.

Suppose that the second plot option is desired: every scan is to be plotted. The averaging period is then arbitrary as far as the program function is concerned, and should be made as large as possible for efficiency's sake (61 scans per period). Then in the example above, each dump contains 320 scans, which represents a much shorter time interval but the same number of data points to be stored and plotted.

B) Storage and Manipulation of Data

The main subdivisions of the program are READ, subroutine REDUCE, and subroutine PLMAT. The latter has entries PLSAV, PLSND, and PLTT. The tape is read in READ, the data are reduced in REDUCE, and data are written to mass storage in PLSAV and PLSND. Later on, PLTT does the plotting.

Upon being read from the tape, data are moved through storage locations as follows:

1. READ: The tape is read by the main program, READ. Every scan is read into STOR, a 40-element array. After each scan, subroutine REDUCE is entered.

2. REDUCE: So long as the current averaging period is still being filled, the contents of STOR are simply copied into columns of ARRAY (a 40 by 64 array) starting at column 4. Then control is returned to READ for a new scan. An averaging period can have up to 61 scans.

Once a scan is read which has an experiment time past the current averaging period, STOR is held in limbo while the contents of ARRAY are processed:

i. The raw data in each row of ARRAY are searched for their minimum and maximum. Their average value is computed, and these numbers are stored in the first three elements of each row of ARRAY.

ii. The raw data are converted to physical units in ARRAY.

iii. Most of ARRAY is copied as is into BRRAY, which is also 40 by 64. Those rows of ARRAY corresponding to unused channels

are eliminated, so BRRAY is more compact, in general. Columns of BRRAY are NREC in length. (NREC is the number of records per dump, since there is one record per useful channel per dump.) This transfer eliminates many logical operations later on.

iv. Contents of BRRAY are printed, if desired.

v. PLSAV is called, to store whatever information is to be plotted, and control is returned to REDUCE.

At this point, the current averaging period has been taken care of, and indices are reset for the next one. STOR is read into column 4 of ARRAY, more scans are read, and the process is repeated.

3. PLSAV: The points to be plotted are stored in CRRAY, a 10240-element array, prior to being dumped to mass storage. CRRAY is implicitly partitioned into NREC sections (one per channel) of RECL words each. Each section, once filled, will constitute one record of the dump.

For plot option 1, there is one point per channel per averaging period. Section 1 of CRRAY---elements 1 through RECL---receives points from channel 1 for averaging periods 1 through RECL; section 2---elements RECL+1 through 2*RECL---receives points from channel 2. Section NREC, the last, receives points from the last channel used. For averaging period NAP, the location in CRRAY for data from channel N is LOC = (N-1)*RECL + NAP. That is, CRRAY(LOC) contains that point. After storing one point per channel in CRRAY, control returns to REDUCE unless CRRAY is full.

Once RECL averaging periods have been completed, the useful portion of CRRAY is full, and the dump is made: NREC records, of length RECL,

numbered consecutively in the index register INDEX, are written by calls to WRITMS. For dump number NDUMP, the index of the record containing data from channel N is IX = (NDUMP-1)*NREC + N.

(Note that, prior to the WRITMS operation, each section of CRRAY is copied into array DUMP, which has RECL elements. DUMP shares memory with array ARRAY from REDUCE, which contains information that is superfluous by the time PLSAV is entered.)

After a dump, control returns to REDUCE, and the new averaging period begins.

For plot option 2, there are many points per channel per averaging period---say 20, for sake of illustration. Then section 1 of CRRAY receives 20 points from channel 1 after the first averaging period, 20 more after the second, and so on with the same true of all sections. If RECL = 320 as in the example cited earlier, 16 averaging periods would exactly fill CRRAY and a dump would be made. If, however, there were 21 points per period, then after the 16th period the following would occur: the first 5 scans are packed into each section of CRRAY, filling them; the dump is made; and then, after indices are reset, CRRAY is refilled from the beginning with the remaining 16 scans. Then control returns to REDUCE.

To summarize, STOR holds data from one scan; ARRAY and BRRAY, from one averaging period; and CRRAY, from one dump. The records written to TAPE8 eventually contain all the information to be plotted in one plot period.

Generally, the time window will end with CRRAY only partly filled. The last dump will then produce "short records" with SRECL words, rather than RECL words. This is accomplished by entering PLSND instead of PLSAV.

C) Plotting

Once the full time-window has been read, plotting begins in entry PLTT. An array must be established for the time axis, which is the y-axis on paper. For plot option 1-(2) the array contains---for each point in the first record---the decimal number of days (hours) from the beginning of the time window. The first 2560 elements of CRRAY (whose original purpose has been served) are reserved for this.

The labels for the time axis--which must be drawn NREC times---are of the form DAY 161 DAY 162... or JUN 10 JUN 11... for plot option 1; or 900 1000 1100... for option 2. These are stored in CRRAY also.

The time axis starts at the beginning of the first day (hour, if option 2) in the time window. Of course the data start wherever the time window starts.

For each channel the complete axes are drawn and labelled first. Labels other than for the time axis come from DRCTV. Then the data records are retrieved by calls to READMS. The index for the Ith record corresponding to channel N is IX = (I-1)*NREC + N. Records are read into array DUMP, which constitutes the x-array for plotting.

The y-array for plotting is BRRAY, which must be constructed. For the first record of a given channel, it is identical to the first elements of CRRAY; for succeeding records CRRAY is augmented by however many days (hours, option 2) correspond to the number of full records already read and plotted. In other words, if RECL points correspond to DPR days (per record) then the y-array for the Ith record is BRRAY(J) = CRRAY(J) + (I-1)*DPR, for J = 1, RECL.

The plot routine LINE plots DUMP versus BRRAY for the first record of the channel in question. Then the second record is read into DUMP, BRRAY is reconstructed, and the next RECL points are plotted. This process continues until the last record has been retrieved and plotted. Then the plot origin is reset and the next channel is processed.

D) Use of the Program

1. Required Input Files

a) TAPE3 contains:

---A table of coefficients (COFS(N, J), J=1, 5) for reduction of VLF data in 26 channels (13 channels of phase information, 13 channels of amplitude information; N = 1, 13). 13 card images, each read in FORMAT(5F10.5)

---A table of integer directives (DRCTV(N, J), J=1, 15) for plotting and handling data for each channel on the field tape. Appendix A explains the table. 40 card-images in FORMAT (2I3, 4A10, 3I3, 3I5, 3I3).

b) TAPE4: the backup tape containing the experiment data

c) INPUT (TAPE5): three card-images with the following variables:

---NFX, NWX, NSCAN, NCHAN, SCAN, YR, IC FORMAT(7I5)

---TBEG, TEND, AVG FORMAT(2I10, I5)

---PRINT, PLLL, ARAN, FACTOR, IDT, SIZE FORMAT(2I5, 2F5.2, 2I5)

Typical values are given in parentheses. Program information:

NFX = number of files on the backup tape (1)

NWX = number of words per record on the backup tape (226)

NSCAN = number of scans per record on the backup tape (15)

NCHAN = number of channels per scan on the backup tape (40)

SCAN = number of seconds between consecutive scans (30)

YR = year in which experiment began (78)

IC = system code

Time window and averaging period:

TBEG (dddhhmmss) = beginning of time window

TEND (dddhhmmss) = end of the time window

AVG = duration of a single averaging period, in seconds (600)

Print and plot options:

PRINT = print option: 0 means no data are to be printed; 1 means print the minimum, maximum, and average value, in each averaging period; 2 means print this plus the scan-by-scan results.

PLLL = plot option: 0 means no plot; 1 means plot the average value in each period; 2 means plot scan-by-scan results.

ARAN = number of inches per day (hour) on the time axis. DEFAULT = 2"

FACTOR = multiplicative scaling factor for plotting. DEFAULT = 1.0

IDT = code for labelling time axis: 0 means "DAY 161 DAY 162 ..."; 1 means "JUN 10 JUN 11 ..." DEFAULT = 0

SIZE = size of paper, in inches (11" or 30") DEFAULT = 30"

2. Other Files Used

a) OUTPUT (TAPE6) provides running commentary on anything unusual on the backup tape, and is used for printed data output.

b) TAPE8: random-access scratch file.

c) PLOT: to be disposed to the online plotter.

3. Time and Memory

The program requires 114,000 (octal) words of core. Processing 1500 backup tape records (about 8 days' data) takes approximately 80 seconds.

4. Miscellaneous

Special note ought to be made of the plotting procedures if PLLL = 2. The averaging periods are just bins for collecting data to be plotted. No time information for individual scans is kept, just the beginning and end of the period. Therefore a problem arises if there are time gaps on the field tapes. All data within an averaging period are plotted from the beginning as if the scans were equally spaced in time, and consecutive. If gaps exist, fewer scans occur in the period. The averaging period is then filled at the end with minimum values. Therefore, CAUTION: if time gaps appear on the field tapes, they will, in general, appear at slightly later times on the plot than they actually should. Moreover, if a single gap runs from one period into the next one, it will appear as two gaps, at the end of both periods.

If this becomes a problem, the averaging period can be shortened to the scan time (AVG = SCAN). This will cause the program exec time to increase considerably.

If PLLL = 2, the number of scans per averaging period should be constant. Therefore, AVG should be chosen so that SCAN divides evenly into it.

The preceding comments in this section do not apply if PLLL = 1.

If it becomes necessary for averaging periods to accommodate more than 61 scans, the dimensions of ARRAY and BRRAY in REDUCE must be increased. The present 40 by 64 size allows for 61 scans and the minimum, maximum, and average values for each of 40 channels. For 100 scans, 40 by 103 would be needed. Also, LIMIT in subroutine REDUCE must be increased, and the dimensions of BRRAY should be adjusted in PLMAT.

If more than 40 channels are required, it is sufficient to increase the dimensions of any arrays which are presently set at 40, and augment the data reduction section of REDUCE.

Writing and reading the random-access file is not particularly time-consuming. A quick test showed that 500 records of 20 words can all be created, written to mass storage, and retrieved in .7 seconds. (For comparison, if these records are also output to the printer, the WRITE operation alone requires an additional 1.5 seconds.) Expanding the record-length to 500 words only triples the time required for retrieval.

APPENDIX A: The Table of Directives

The table of directives, DRCTV (see section III-D-1-a) is a 40 by 15 array. The 15 elements of each row have the following meanings.

1 (I3) Channel index (1-40). Channels are numbered 0-39, but indexed 1-40 because of the FORTRAN subscript requirement. No program function, only used to keep the table in order.

2 (I3) Sensor number (1-40) associated with a given type of instrument, which could be plugged into any channel. Used for data reduction in REDUCE.

3 (A10) 10 characters used to label the data-axis of the plot.

4 (A10) 10 characters giving the units of the data-axis label.

5,6 (2A10) 20 characters identifying the type of measurement being plotted.

7 (I3) Data disposition directive: 0 means ignore all the data from this channel; 1 means process it. In the channel containing y-component magnetometer data, 2 means compute the horizontal component and store it there.

8 (I3) VLF data reduction directive: refers program to correct elements of COFS.

9 (I3) Reserved for riometer subtraction option.

10 (I5) Maximum data value to be plotted.

11 (I5) Minimum data value to be plotted.

12 (I5) Total number of inches on the data-axis for this channel.

13-15 Not used.

APPENDIX B: Dumps of a Typical Record

The following is a character dump of the first 530 characters (53 words corresponding to 2 full scans) of the first record on a field tape. Spaces appear in the record exactly as shown.

"CL010<01<54<07CL 030782-00005+ 9516+ 0004+ 9517+ 0004+ 9510+ 0005+ 9524+ 0005+ 9512+ 0002+ 9519+ 0004+ 5298+ 0003+ 5305+ 0003- 4337+ 0810-10007- 0012+ 2991+ 0016+ 3038+ 0757+ 6724+ 3296+ 0003+ 0002+ 0002+ 7367+ 0003+ 0002+ 3856+ 6472- 0050+ 3424- 0205- 0019+ 1338"CL010<01<54<37CL 030782-00005+ 9516+ 0004+ 9517+ 0004+ 9510+ 0005+ 9524+ 0005+ 9512+ 0002+ 9519+ 0003+ 5298+ 0003+ 5305+ 0003- 4337+ 0811-10017- 0012+ 2882+ 0016+ 3038+ 0766+ 6652+ 3201+ 0003+ 0002+ 0002+ 7366+ 0003+ 0002+ 4011+ 6596- 0051+ 3424- 0200- 0035+ 1342

The following is an octal dump of the first 31 words (2 full scans) of the backup-tape record which was made from the field tape whose character dump is given above. 60-bit words are separated by spaces for clarity.

646464640000000074076 640000011051604572570000012060266011610403013320470420140546
023421206027201161050130132004704101405570234210054171011610302607620470414010361
023732401161340000140247402047050012403602371520555020124440023420604704101161020271016047041411610202532400553040000062025150000014640000230241364000000000000
640000011051604573150000012060266011610403013320470420140546023421206027201161050130132004704101405570234202054171011610302607620470414010361023732601161340000140247404047050012403602371740554360124301023420604704101161020271014047041411610202537260554020000063025150000014400000430241374000000000000

The first word contains the recognition character 64646464 plus the octal number 74076, which equals 30782 to the base 10 (the fixed data). In the second word, $1105160457257_8 = 78010015407_{10}$ which is the first experiment time. The third word should be broken down into bits and reconstructed in thirds:

$0000012060266011610 4_8$ equals

$000000000000000001010000110000010110110000001001110001000100_2$

The first 20 bits converted to decimal give 5; the second 20 give 49516; and the third 20 bits give 40004. This translates to -5, +9516, and +4, which can be seen from the character dump to be the raw data values of the first three channels of the first scan.

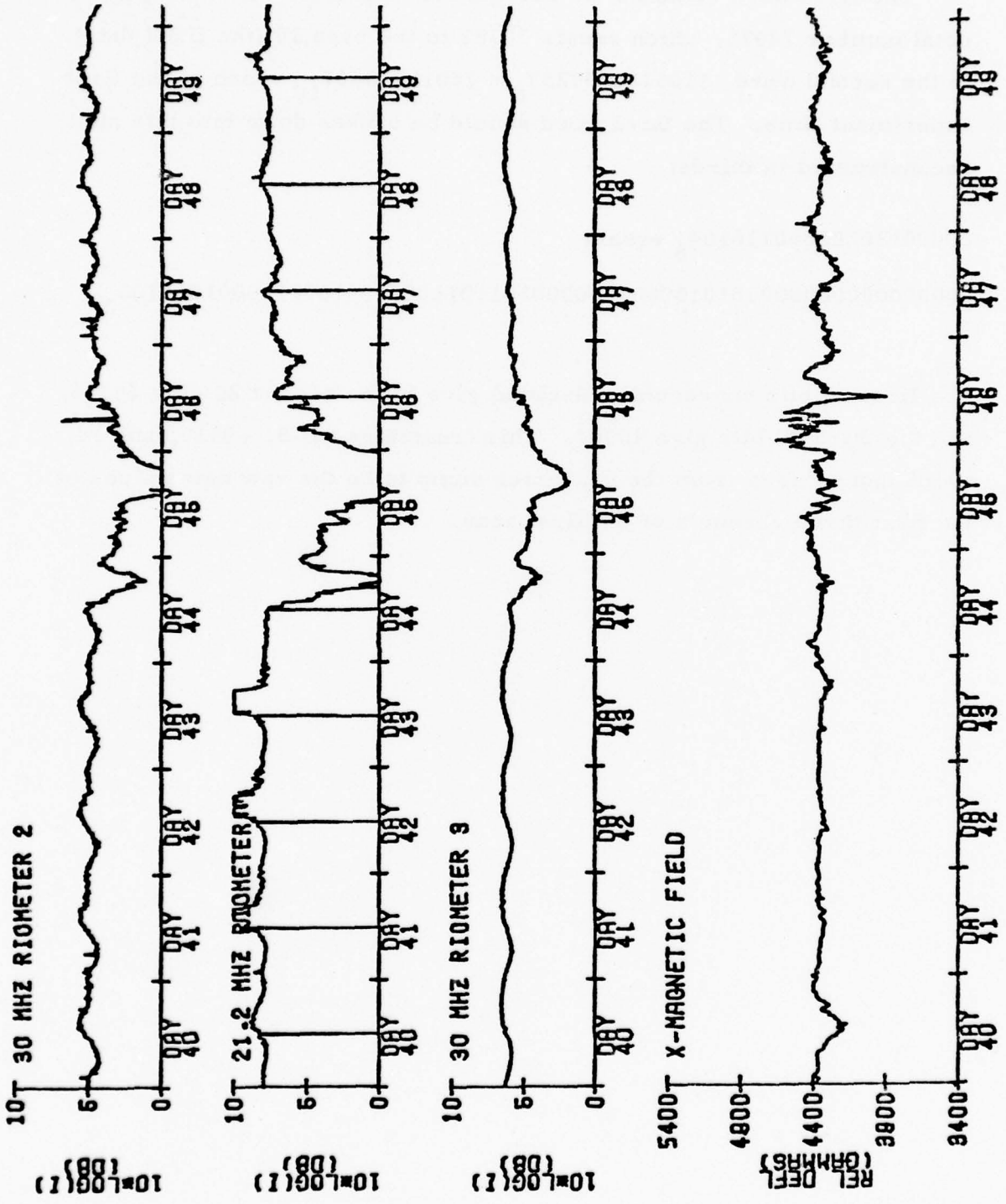

APPENDIX C: A Portion of a Typical Plot

VII. IONOSPHERIC PULSE REFLECTIONS

1. Introduction

Substantial modifications were made to an existing program which had been written to calculate the effects of different model ionospheres on VLF signals reflected from them. These effects are determined from the amplitudes and phases of the four complex reflection coefficients, $_{||}R_{||}$, $_{||}R_{\perp}$, $_{\perp}R_{||}$, and $_{\perp}R_{\perp}$. The first subscripts refer to the polarization of the incident field with respect to the plane of incidence (the vertical plane containing the wave-normal), and the second refer to the polarization of the reflected field. In an anisotropic medium ($\vec{B} \neq 0$), $_{||}R_{\perp}$ and $_{\perp}R_{||}$ are generally not zero because of Faraday rotation of the plane of polarization.

In the case at hand, a fullwave treatment was used to get the phases of $_{||}R_{||}$ and $_{||}R_{\perp}$, given the ground distance from transmitter to receiver, as a function of the angle of incidence. For nonuniform ionospheres, these are found by successive integration of four simultaneous first-order differential equations (relating components of the electric and magnetic field) over regions in which the ordinary and extraordinary indices of refraction vary. The desired quantities were the stationary phases of $_{||}R_{||}$ and $_{||}R_{\perp}$—that is, the angles of incidence at which the phases reach their maximum values. This is sufficient to approximate the "path" of the reflected wave to a satisfactory extent. The amplitudes of the reflection coefficients at stationary phase and the group heights were also to be determined.

2. Program Description

The program is written so that a range of frequencies is considered. For each frequency, the reflection coefficients are calculated (in

subroutine BLBOX) as a function of the angle of incidence, φ, and the phases are referred to some specific point, usually the location of the transmitter. The phases, originally determined modulo 2π, are adjusted (in subroutine STAFAZE) by the addition of multiples of 2π to remove artificial discontinuities. Then a term is added to refer the phase to the receiver rather than the transmitter. The resulting phases, regarded as a function of φ, show a maximum somewhere between $\varphi=0^\circ$ and $\varphi=90^\circ$.

To find the stationary phase angle for each reflection coefficient, the table of phases is searched for its greatest value. An interpolation procedure is used to generate a new table including only the region of the maximum. This in turn is searched for its maximum, which should be very close to the desired maximum. As a check, the reflection coefficients are redetermined at three points straddling the peak and the actual maximum is found by interpolation using these three points. This procedure locates the value of φ corresponding to stationary phase within, at least, $.05^\circ$. The values of the amplitude, phase, and φ for each reflection coefficient are stored, and the program proceeds with the next frequency.

Occasionally when the steps in φ (PSTEP) are too large, consecutive phases actually differ by more than 2π. In such a case, an ambiguity can arise in STAFAZE resulting in the addition of the wrong multiple of 2π. The program recognizes this condition and repeats its calculations with smaller steps. This is more likely to happen for higher frequencies than for lower ones.

The range of φ to be searched for the maximum in the phase angles is read in at the beginning. If the maximum lies outside this

region, the program prints a comment to that effect and proceeds with the next frequency.

If one needs the values of the reflection coefficients only at a single angle of incidence, one can set PSTEP equal to zero. In this case, the stationary phase section is bypassed.

If desired, the group heights for the two cases are calculated in subroutine GRPHT, after the stationary phases have been determined for all frequencies. If a single φ is used, so that stationary phases are not found, this section is bypassed.

Another available option is to plot the magnitude of the reflection coefficients at stationary phase, and/or the group heights, as a function of frequency. If stationary phases are not found, the reflection coefficients generated for the given φ are plotted.

It can happen, for model ionospheres with profiles containing particularly large gradients, that the phases do not increase and decrease monotonically on either side of the absolute maximum. In fact, it is possible to get "ledges" (inflection points) or even subsidiary maxima in the table of points representing the phases. In such cases, the peak-location procedure can give erroneous results or, more likely, end up mistaking this problem for a 2π ambiguity somewhere. In the latter case, the program cuts the step size and tries again. It is not clear whether the local maxima are due to actual physical circumstances, or rather to numerical procedures in the supplied routines in BLBOX which are not sufficiently accurate for the sorts of ionospheric models encountered.

3. Use of the Program

The required input data are in the original format, except that the last card has been added to allow the group height calculations and the plotting to be optional. This card reads three integer parameters, NPLOT, GRP, and MPLOT in format 3I5. If NPLOT is not zero, the stationary phase plot is drawn. If MPLOT is not zero, the group height plot is done. If GRP is not zero, the group heights are calculated. If any of these parameters is zero, the corresponding section is skipped. If GRP=0, MPLOT is automatically set to zero.

A list of input parameters follows:

Quantity	Format	Explanation
DG	F10.4	transmitter-receiver distance (km)
CMNT(1,K),K=1,6	6A10	general comment
CMNT(2,K),K=1,6	6A10	comment
HN0, DHN	2F8.2	starting height, height interval for electron density profile (km)
ENL(K),K=1,KN	8F10.5	electron-density profile
CMNT(3,K),K=1,6	6A10	comment
HNU0, DHNU	2F8.2	starting height, height interval for collision-frequency profile (km)
ENUL(K),K=1,KNU	8F10.5	collision frequency profile
HREF	F10.2	reference height (km) (generally zero)
HT(1),NO(1),N1(1)	F10.2,2I5	starting height for integration (km); number of integration steps per wavelength (in units of 100); step multiplier

HT(2)	F10.2	stopping height for integration (km)
F, FH, DIP, AZ, PHI	5F10.4	starting frequency; gyro frequency; dip angle; azimuth; starting angle of incidence
FEND, FSTEP, PEND, PSTEP	4F10.4	last frequency; frequency interval; last angle; angle interval
NPLOT, GRP, MPLOT	3I5	see comments above

VIII. THE IMPROVEMENT FACTOR FOR THE ARRESTED SYNTHETIC APERTURE

1. Introduction

Program ASAR computes the improvement factor for the arrested synthetic aperature radar (ASAR). The ASAR processing combines displaced phase center antenna (DPCA) processing with doppler filtering to enhance the improvement factor.

2. Problem Background

Suppose an aircraft A (velocity v) carrying a radar antenna, sees a target in its main beam at an angle θ_o (Fig. 1.). At the same time a large stationary object G (ground) appears in a side lobe of the antenna pattern at angle θ. A portion of the ground G has an apparent approach speed of v cos θ, whereas, a stationary target in the mean beam approaches at v cos θ_o. It is possible that the target T has the same apparent speed as the portion of ground G. Thus conventional doppler filtering which suppresses the main beam stationary target cannot suppress side lobe ground reflection. One method of suppressing ground clutter is ASAR processing.

3. ASAR Processing

3.1 General Description

In ASAR processing, the antenna beam used for target detection is assumed to be formed by a combination of two antenna arrays, array A1 and array A2. (See Fig. 2). Each antenna array is a linear array of elements. These linear arrays are aligned along the flight path (velocity v). Their phase centers are separated by a distance d. The signal received by each antenna array is processed by identical bandpass filters. The outputs of both filters are then

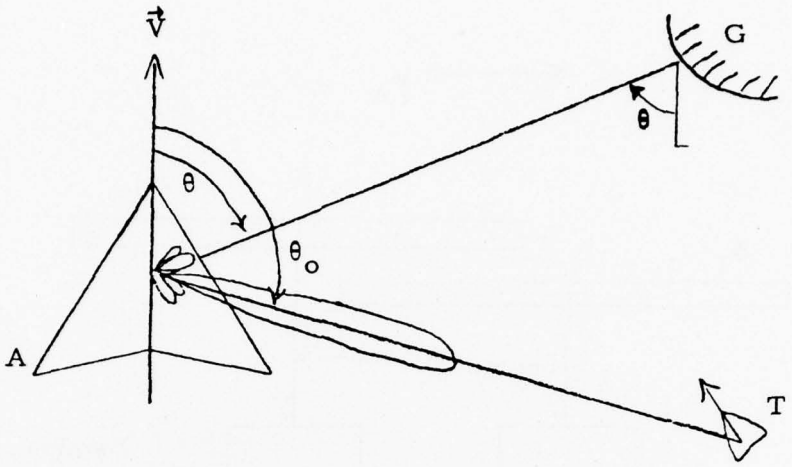

Figure 1. Problem Geometry

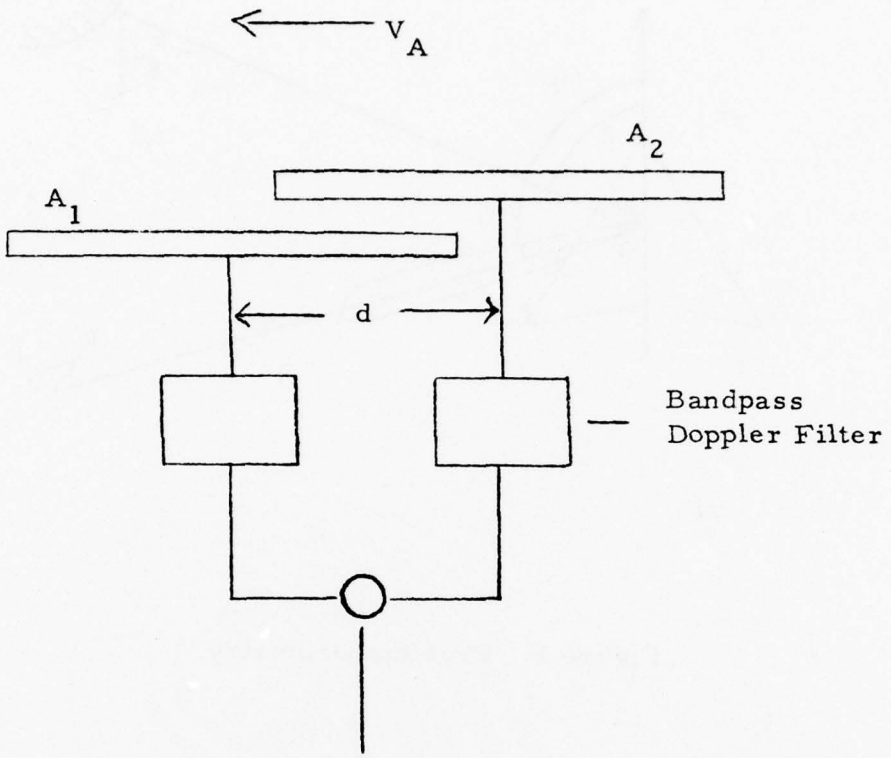

Fig. 2

respectively weighted by complex constants (processing constant A, and processing constant B) and summed. This summed coherent signal is then detected to provide an appropriate detection statistic.

The signals from both arrays A1 and A2 are in the form of pulses. The pulses from array A2 are emitted at a slightly later time τ then the pulses from array A1. In ASAR processing, the delay time τ is chosen to be the ratio between the separation distance d between corresponding array elements and the aircraft velocity v ($\tau = d/v$).

Although both arrays are identical, the patterns produced by each array are different. This difference is due to the fact that the antennas are at different locations in the airplane and, therefore, are subjected to different reflection characteristics.

By appropriately choosing the processing constants A and B, it is possible to partially reduce the ground clutter (reflection from ground) in comparison to the signal (reflection from target). Indeed, if the patterns from both arrays were the same, it would be possible to cancel all ground clutter by choosing the processing constant B to be the negative of processing constant A. This cancellation of ground clutter is due to the fact that the ground is stationary. The target signal, however, is not cancelled because it is moving.

3.2 The Signal

The two way complex voltage $E_i(\theta)$ received by the i'th array ($i = 1, 2$) due to reflection from the target is a function of the line of sight angle θ_o between the direction of flight path v and the line of sight joining the aircraft A and the target T.

The net complex voltage output E after filtering and weighting is a weighted coherent sum of the respective complex voltages $(E_1(\theta_o), E_2(\theta_o))$ received at each array, provided that the doppler frequency ω_d is within the frequency band $(\omega_c - \Delta\omega, \omega_c + \Delta\omega)$ of the filter:

$$E = \begin{cases} A E_1(\theta_o) + B E_2(\theta_o) e^{j\omega_o \tau}, & \omega_c - \Delta\omega \leq \omega_d \leq \omega_c + \Delta\omega \\ 0, & \text{otherwise} \end{cases}$$

The doppler frequency ω_d is the doppler frequency associated with the radial velocity between aircraft and target. The delay time τ has been previously defined.

3.3 Ground Clutter

In addition to the target reflection, there is ground reflection (ground clutter). The coherent two way complex voltage E_c due to an increment of ground at a line of sight angle θ is

$$E_c(\theta) = (A E_1(\theta) + B E_2(\theta))\, d\theta$$

The two way complex voltage received by different increments of ground are assumed to be incoherent with respect to one another. Therefore, the net ground clutter power C is the sum of the ground clutter power due to each ground increment.

If the clutter power C is normalized to the power C_0 from a single element, we obtain:

$$C/C_0 = \frac{1}{\pi} \int_{\theta_c - \Delta\theta}^{\theta_c + \Delta\theta} |E_c(\theta)|^2 \, d\theta \quad .$$

The clutter angle θ_c is the line of sight angle that corresponds to a doppler frequency ω_c equal to the center frequency of the filter:

$$\omega_c = \frac{4\pi v_A}{c} f_R \sin \theta_c \quad .$$

The frequency f_R is the carrier frequency of the radar. The angle interval $(\theta_c - \Delta\theta, \theta_c + \Delta\theta)$ corresponds to the frequency band $(\omega_c - \Delta\omega, \omega_c + \Delta\omega)$ of the filter:

$$\omega_c \pm \Delta\omega = \frac{4\pi v_A}{c} f_R \sin (\theta_c \pm \Delta\theta) \quad .$$

3.4 Noise

The noise level N_i from each antenna is the sum of the noise levels N_0 of each of the P array elements:

$$N_i = P N_0$$

The antenna noise N_i in each antenna is limited by the doppler band pass filter of frequency width $2\Delta\omega$. The noise output $\overline{N}_i$ of each bandpass filter is:

$$\overline{N}_i = \frac{2\Delta\omega}{\omega_{prf}} N_i \quad .$$

After passing through the band pass filter, the noise $\overline{N}_i$ is acted on by the processing constant C_i ($C_1 = A$, $C_2 = B$) thus producing noise N_i':

$$N_i' = |C_i|^2 \overline{N}_i, \; C_1 = A, \; C_2 = B \quad .$$

The noise produced in antenna 1 is incoherent with respect to the noise produced in antenna 2. Therefore, the net noise output N is the sum of the noise output N_1 produced by the first antenna and the noise output N_2 produced by the second antenna:

$$N = N_1' + N_2' \quad .$$

It is convenient to express the above net noise out in terms of the ratio η of the noise power N_0 to clutter power C_0 produced by one array element:

$$\frac{N}{C_0} = \frac{2\Delta\omega P\eta}{\omega_{prf}} \left[A^2 + B^2\right]$$

3.5 Maximization of Improvement Factor

The improvement factor I is the ratio of the signal to clutter plus noise ratio S/(C+N) and the reference signal to clutter ratio S_0/C_0 due to one array element:

$$I = \frac{S/(C+N)}{S_0/C_0} \quad .$$

The signal S, clutter and noise terms N are positive quadratic functions in the processing constants A and B. Therefore, the improvement factor I is the ratio of two positive quadratic forms in the processing constants A and B:

$$I = \frac{C^+ \overline{A}\, C}{C^+ \overline{B}\, C}, \quad C = \begin{pmatrix} A \\ B \end{pmatrix} \quad .$$

It is desired to maximize the improvement ratio I with respect to the processing constants A and B. If the positive definite matrix $\overline{A}$ is of the form $A = a\, a^+$, and the matrix B is positive definite then the maximization of the ratio is given by:

$$I = a^+ \overline{B}^{-1} a \quad .$$

4. Program ASAR

Program ASAR computes:

1. The improvement factor I as a function of the radial target velocity.

2. The two way gain functions $G_i(\theta)$ for each antenna at a given line of sight angle θ vs. the doppler frequency ω_d. The two way gain function is related to the two way complex voltage as follows:

$$G_i(\theta) = 10 \log |E_i(\theta)|^2 \qquad i = 1, 2$$

Plots of the above are also made.

Program ASAR is divided into the following parts:

1. A subroutine 'PATTERN' for the computation of the two way complex voltage pattern due to a linear array of elements.

2. A subroutine 'IMPROVE' for the computation of the improvement factor.

IX. COMPUTATION OF THE SPECTRUM OF AN ENSEMBLE OF SIGNALS

1. Introduction

Program "SPECTRM" computes the spectrum of an ensemble of signals. The signals are constructed from the data obtained from a tape.

2. Reading of Tape

The tape consists of a large number of files. Each file consists of several records. The data on a group of files constitutes the information needed to construct each signal.

3. Unpacking of Data

The data tape is a 9 track tape. One track is for parity and 8 tracks are for storage of packed words. The words are stored across the tape; thus each packed word consists of 8 bits.

The CDC word is a 60 bit word. Fifteen packed words (characters) are read into a pair of CDC words. Seven packed words plus one half a packed word are contained in the first member of the pair of CDC words. The remaining half of the last packed word is contained in the first part of the second CDC word.

These 15 packed words that are stored in 2 CDC words are then unpacked into 15 CDC words. Each of the 15 CDC words then contains a packed word, that is right justified. The 15 CDC words are then divided into 5 triplets. Each triplet is used to form a number. The number is the bit string formed by three contiguous packed words. The first pair of CDC words at the beginning of a file contains the identification (year, day, test no. and file no.) for the file.

4. Program Spectrum

Program SPECTRM is divided into 6 parts:

1. Reading of the data tape.
2. Unpacking of data obtained from the tape.
3. Construction of the ensemble of signals.
4. Averaging over the ensemble of signals to produce one averaged signal.
5. Computation of spectrum of the averaged signal that lies within a prescribed time window. (The spectrum is computed using the fast Fourier transform method.)
6. Computation of amplitude and phase of spectral components of the time limited averaged signal.

The program is constructed as a set of nested loops. The outermost loop governs the reading in of files. The second loop (going inward) governs the processing of a record. The third loop governs the unpacking of a pair of words.

X. MAXIMIZATION OF ANTENNA GAIN

1. Introduction

Program ANT was designed for the maximization of antenna gain in curtain arrays. The current distribution in the antenna satisfies a system of integral equations. This set of integral equations is solved using a matched point method taking the classical King Mack Sandler functions as a basis.

The antenna gain is a function of the current distribution and is computed in the standard way. The current distribution is a function of the geometry of the array. Therefore, the antenna gain is also a function of antenna geometry. In particular, the gain depends on the element lengths and inter-element spacing.

The antenna gain may be maximized with respect to a set of parameters. This maximization may be achieved using the Hooke-Jeeves algorithm. In particular, the maximization of gain may be achieved with respect to element lengths and inter-element spacings.

2. Integral Equation for the Current Distribution

2.1 Derivation

The current distribution in an antenna may be derived from Maxwell's equation relating the radiated field-A, to the current distribution J:

$$\nabla^2 A(r,t) - \frac{1}{c^2} \frac{\partial^2 A(r,t)}{\partial t^2} = -4\pi J(r,t) \qquad (1)$$

The above equation may be Fourier transformed with respect to time

AD-A076 150 ARCON CORP WALTHAM MA F/G 20/14
MATHEMATICAL ANALYSIS AND PROGRAMMING AS APPLIED TO ELECTROMAGN--ETC(U
JUN 79 J O'BRIEN , I KOLTUNOV F19628-76-C-0310
UNCLASSIFIED RADC-TR-79-146 NL

2 OF 2
AD
A076150

END
DATE
FILMED
11-79
DDC

to give the following equation:

$$\nabla^2 A(r,\omega) + k^2 A(r,\omega) = -\frac{4\pi}{c} J(r,\omega) \quad . \tag{2}$$

For free space, the above differential equation may be converted to Maxwell's equation in integral form:

$$A = \int G(r,r') J(r') \, dr' \quad . \tag{3}$$

The free space Green's function is:

$$\begin{aligned} G(r,r') &= e^{ikR}/R \\ R &= |r - r'| \quad . \end{aligned} \tag{4}$$

If the antenna consists of parallel wires oriented along the z-axis (e.g. curtain array) then the above integral (3) may be decomposed into integrals along each wire:

$$A(r) = \sum_j \int G(r, z_j') I_j(z_j') \, dz_j' \quad . \tag{5}$$

The index j indexes the elements of the array.

The A-field A_i at the i'th element, is given by:

$$A_i = \sum_j \int G_{ij}(z, z') I_j(z') dz' \quad . \tag{6}$$

The Green's function G_{ij} still has the same form as (4). However, the distance R is the distance between the two points z and z' located on element i and j respectively.

The form of the A-field may also be deduced from a combination of symmetry considerations and boundary conditions. Again, if the antenna consist of elements oriented along the z-axis, then the above Maxwell's equation (2) in differential form reduces to:

$$\left(\frac{d^2}{dz^2} + \beta^2\right) A(z) = 0 \quad , \quad \beta = |k| \quad . \tag{7}$$

The above equation has a sinusoidal solution with arbitrary phase and amplitude:

$$A(z) = a \cos \beta z + b \sin \beta z \quad . \tag{8}$$

We shall assume that the current satisfies the following symmetry condition:

$$I(z) = I(-z) \tag{9}$$

The same symmetry must be inherited by the A-field:

$$A(z) = A(-z) \quad . \tag{10}$$

This symmetry can be obtained by imposing the following restriction on the above solution:

$$A(z) = a \cos \beta z + b \sin \beta |z| \quad . \tag{11}$$

Finally, the electromagnetic field must satisfy appropriate boundary conditions. Namely, the tangential E-field must be continuous at the wire surfaces of the antenna. The above boundary condition allows the A-field at the i'th wire surface to be expressed in terms of the gap voltage V_i of the i'th antenna:

$$A_i(z) = -j \frac{4\pi}{\eta} \left(C_k \cos \beta z + \frac{1}{2} V_k \sin \beta |z| \right) \quad . \tag{12}$$

The intrinsic impedance of the surrounding medium is η. Equating the two expressions (6, 12) for the A-field at the surface of the i'th element, we obtain the system of integral equations for the current distribution $I_j(z)$.

2.2 Method of Moments

The method of moments is a method of finding an approximate solution to a system of integral equations. In the method of moments, the current is expanded in terms of a basis:

$$I_j(z') = \sum_{n=1}^{N} I_{jn} J_n(z') \tag{13}$$

The system of integral equations (6, 12) for the current distribution then becomes:

$$\begin{aligned} \sum_{j,n} Q_{ijn}(z)\, I_{jn} &= A_i(z) \\ Q_{ijn}(z) &= \int G(z,z')\, J_n(z')\, dz' \quad . \end{aligned} \tag{14}$$

We may choose a different class of functions W_m (weighting functions) that also span the same space as the basis J_n. Taking the inner product on both sides of the above equation (14) with the m'th weighting function, we obtain the matrix equation:

$$\sum < W_m, Q_{ijn} > I_{jn} = < W_m, A_i(z) > \tag{15}$$

There are two classes of weighting functions that are commonly used:

1. The weighting functions that are the basis functions ($W_m = J_m$) (Galerkin method).
2. The weighting functions that are Dirac delta functions (matched point or collocation method).

In the matched point method the weighting functions are chosen to be delta functions:

$$W_m = \delta (z - z_m) \quad . \tag{16}$$

In this case the above equation (15) becomes:

$$\sum_{j,n} Q_{ijn} (z_m) I_{jn} = A_i (z_m) \quad . \tag{17}$$

We see that in the matched point method, both sides of the equation (17) are matched at a sufficient number of points z_m so as to be able to determine the current coefficients I_{jn}.

A good set of basis functions are the King, Mack and Sandler functions:

$$
\begin{aligned}
J_1 &= \sin\beta(h - |z|) \\
J_2 &= \cos\beta z - \cos\beta h \\
J_3 &= \cos\left(\frac{1}{2}\beta z\right) - \left(\cos\frac{1}{2}\beta h\right) \\
\beta &= 2\pi/\lambda \\
h &= \text{height of dipole.}
\end{aligned}
\tag{18}
$$

For an antenna in free space, the far field radiation A may be determined from the current distribution using Maxwell's equation in integral form (5).

Once the A-field is determined, the E-field and H-field may be simply determined:

$$
\begin{aligned}
E &= j\omega A \\
H &= \frac{1}{\omega}\nabla \times A \quad .
\end{aligned}
\tag{19}
$$

The Poynting vector S may be determined from the E and H field:

$$
S = E \times H \quad . \tag{20}
$$

The Poynting vector may be thought of as the amount of power P flowing in a particular direction $\hat{U}$.

$$S = P\,\hat{U} \quad , \quad P = |S| \quad . \tag{21}$$

The power flow P depends on the direction $\hat{U}$. The direction may be specified in terms of spherical angles (θ, φ):

$$\hat{U} = \cos\varphi \sin\theta\, \hat{i} + \cos\Phi \cos\theta\, \hat{j} + \sin\Phi\, \hat{k} \quad . \tag{22}$$

The total power P radiated from the antenna is the integral of the power flow $P(\theta, \varphi)$ over all directions:

$$P_T = \int 2\pi\, d\varphi\, d\theta \sin\theta\, P(\theta, \Phi) \quad . \tag{23}$$

The antenna pattern $G(\theta, \Phi)$ (gain pattern) is the normalized power flow:

$$G(\theta, \varphi) = P(\theta, \Phi)/(P_T/4\pi) \quad . \tag{24}$$

The gain $G(\theta, \varphi)$ in a particular direction (θ, Φ) is the ratio between

the actual power flow $P(\theta, \varphi)$ in that direction and the power $P_T/4\pi$ radiated in that direction by an equivalent isotropic antenna. By an equivalent isotropic antenna, we mean an isotropic antenna that radiates the same total power as the antenna in question.

A parameter that characterizes the antenna pattern is the front to back ratio. The front to back ratio is the ratio between the maximum gain and the gain in the opposite direction.

2.3 Maximization of Gain

The antenna gain may be considered to be a function of a certain set of variables. In particular, the gain may be considered to be a function of the element lengths and inter-element spacings.

There are several methods for finding the maximum of a function of several variables. One such method is the Hooke-Jeeves (HJ) algorithm. This method has the advantage of not having to supply the gradient of the function. The HJ method is a systematic searching method for finding of the maximum. The search begins at a base point b_1. A local search (exploration) is established about the base point b_1. This local search consists of changing each independent variable x_i by a prescribed step size δ_i. Each variable is first increased then decreased by the step size. If a better point is found, it is adopted as the new base point. If a better point is not found, then the local search is repeated for a constricted domain (each prescribed step size is halved). The algorithm is terminated when one of the prescribed step sizes falls below a critical value.

Assuming that a better base point b_2 is established, and reasoning that if a similar exploration were conducted about base point b_2 as

from base point b_1, the results are likely to be the same, a local search about the second base point b_2 is omitted. Instead, a temporary base point t_2 is established: This temporary base point is in the direction of b_1 to b_2, but of twice the distance from b_1 to b_2:

$$t_2 = b_1 + 2 (b_2 - b_1) \quad .$$

A local search is carried out about the temporary base t_2 with the initial step sizes. If a better point is found than the base point b_2, this point is established as the third base point b_3. We then proceed in exactly the same fashion for the third base point b_3 as for the first base point b_1.

If a better point is not found, then a retreat back to the second base point b_2 is made. We then proceed in exactly the same way for base point b_2 as for the first base point b_1.

2.4 Program ANT

Program ANT is a program that is based on the matched point method for solving the set of integral equations for the current distribution. The three King Mack Sandler functions were chosen as a basis. Using the Hooke-Jeeves algorithm, the gain is maximized with respect to several sets of independent variables. One such set of independent variables is the set of element lengths and inter-element spacings. In addition, the following quantities are computed at the

maximum point:

1. The driving point admittance of the antenna.
2. The relative power in the termination.
3. The standing wave ratio.
4. The absolute directivity.
5. The front to back ratio.

10. REFERENCES

1. C.J. Drane, "On the Three-Term Theory for Analyzing Thin Cylindrical Dipole Antennas," AFCRL-72-0744, Dec., 1972, Physical Sciences Research Papers, No. 523.

2. Wilde and Beighller, "Foundations of Optimization," Prentice-Hall, 1967.

3. R.W.P. King, R.B. Mack and S.S. Sandler, "Arrays of Cylindrical Dipoles," University Press, 1968.

XI. DETECTION AND TRACKING OF LOW FLYING TARGETS BY GROUND BASED RADARS

1. Introduction

The detection and tracking of low flying targets by ground based radars is hampered by various effects such as terrain screening, receiver and environmental noise, ground clutter, bird clutter and multipath. A computer model has been developed to simulate the performance of a ground based radar so as to include the effects of terrain screening, bird clutter, ground clutter, Raleigh distributed noise, multipath and surface roughness.

The analysis of the tracking simulation proceeds on the basis of a target penetrating the radar coverage along a path indicated by the dashed line on Fig. 1. The path is identified by the distance of closest approach SD and the target is located along the path by its distance from the point of nearest approach. As the target penetrates from the right, the radar range equation is used to compute the signal to noise ratios (S/N) and the noise to clutter ratios (N/C). These ratios depend upon the characteristics of the radar, the electromagnetic scattering cross section of the target and environmental parameters (terrain features, weather, noise, electromagnetic interference).

2. Analysis of Target Detection Procedure

The signal to noise ratio is given by the following expression, which may be derived from the radar range equation

$$(S/N) = P_T (\lambda^2) G_A^2 \, FUMF (V_R) \cdot \sigma_T (\theta) F_{ML}^4 (R_A)/((4\pi)^2 R_A^4 \cdot N_o) \qquad (1)$$

where P_T is maximum power of compressed pulse, λ is wavelength,

G_A is one way gain of transmit receive antenna, FUMF is MTI filter function, V_R is radial velocity of target, θ is range of target with respect to y axis, $\sigma_T(\theta)$ is target cross section, R_A is range of target from radar, F_{ML} is function for specular multipath, N_o is total noise power (Raleigh distributed).

The noise to clutter ratio (N/C) is given by

$$N/C = (S/C)/(S/N) \tag{2}$$

where signal to clutter ratio (S/C) is given by

$$(S/C) = F_{ML}^4 (R_A) \cdot X_{MTI} (N_H) \sigma_T (\theta) FUMF (V_R)/[\sigma_{MED} \cdot R_A \cdot \theta_B \cdot C \cdot \tau/2]$$

Here X_{MTI} is clutter improvement due to MTI filter, σ_{MED} is median cross section of log-normal clutter per unit surface area, θ_B is antenna beamwidth in elevation plane, C is velocity of flight, τ is compressed pulse width.

The probability of detection P_{DT} is calculated at a number of points on the target trajectory. The calculations are performed using formulas derived by Fante[3].

The probability of false alarm (P_{FA}) is the probability that the received signal exceeds some threshold level Y_o when there is no target present. Fante[3] has shown P_{FA} may be approximated by the expression:

$$P_{FA} = \frac{1}{2} \operatorname{erfc} \left[\frac{1}{2^{3/2} \sigma_o} \ln \left(\frac{2(N/C) Y_o}{N_H} \right) \right] \tag{3}$$

where erfc (z) is complementary error function, N/C is noise to clutter ratio, N_H is number integrated per scan, σ_o is standard deviation of clutter cross section per unit surface area.

By fixing P_{FA} at a given value equation (3) is solved numerically for the threshold Y_o. Equation (3) was solved using Wegstein's iterative method[4].

Fante[3] has also shown that for large (S/N) ratios the probability of detection P_{DT} of a target with log-normal clutter that varies from scan-to-scan and Raleigh noise that varies from pulse-to-pulse is given by

$$P_{DT} = \left(1 + \frac{1}{N_H(S/N)}\right)^{N_H - 1} \exp\left[\frac{Y_o}{1 + N_H(S/N)}\right] \qquad (4)$$

Computer program PDT uses equations (1) through (4) to calculate P_{DT} for a given P_{FA} at a number of points along the target's trajectory.

3. Simulation of Target Tracking

In order to simulate the radar tracking of aircraft, it is necessary to know: (1) the probability of detection as a function of radar parameters and environmental conditions; (2) the probability that the target is visible due to terrain screening effects; (3) algorithms for monitoring target track together with appropriate processing to provide accurate estimates of target position and speed in the presence of false targets (bird clutter).

The calculation of the probability of detection (P_{DT}) for a given probability of false alarm P_{FA} includes the effects of target fluctuations, noise, clutter, multipath and surface roughness. In order to obtain realistic simulations of target tracking, the effects of terrain screening must also be included.

In the process of radar tracking of a target, two sets of information are of value: (1) the state of the system (target position and velocity) and (2) the future state of the system. The observations of the system are corrupted by noise. The optimum estimate of a set of observations may be obtained by passing the data through a filter.

The simplest filter model is used for tracking, i.e. the fading-memory (exponential) polynomial filter. The effects of association and correlation are neglected. The tracker contains a fixed gain, non-adaptive α-β filter and initiates track on two hits out of three looks. Track is maintained on three hits out of five looks. The simplest case is considered, where the tracker gives no report if there is no hit.

The computer simulation of the detection and tracking of aircraft proceeds in the following manner:

1. A target trajectory is considered as shown in Fig. 1. For given radar parameters and given environmental conditions the probability of detection $P_{DT}^{(K)}$ and the probability of target visibility $P_V^{(K)}$ are calculated at a number of points (R_K, Q_K) along the target trajection.

2. Several thousand target tracking simulations are calculated. In each simulation the following steps are performed:

(a) a uniformly distributed random number $h^{(K)}$ is generated for each target position.

(b) If $P_{DT}^{(K)} \cdot P_V^{(K)} \geq h^{(K)}$, a hit is declared at position (R_K, θ_K); otherwise, the look is declared a miss.

(c) Since there are uncertainties in the measurement of radar range R and azimuth θ, two quantities R and θ may be considered as Gaussian distributed random variables with mean values R_K, θ_K and standard deviations Δ_R, Δ_θ. The standard deviations may be calculated from the formulas given by Barton[6].

(d) The hit or miss report for each point on the trajectory together with the variables R_K, θ_K are fed into the α-β tracking filter. The tracker yields at each point on the trajectory (R_K, θ_K) a report with estimates $(\hat{R}_K, \hat{\theta}_K)$ or, no report.

(e) For each simulation, the absolute errors $R^E = (R_K - \hat{R}_K)$, $\theta^E = (\theta_K - \hat{\theta}_K)$ are calculated. Errors in speed are also calculated.

3. These errors are appropriately summed over the number of simulations and divided by the number of track reports to find their corresponding mean values. If there is no track report in a given simulation, the errors are assumed to be zero. Also the variances in the corresponding errors are calculated.

4. Results and Conclusions

On Fig. 3, the effects of multipath are suppressed. The curve labeled no clutter corresponds to σ_{MED} = -54 dB and the curve labeled clutter corresponds to σ_{MED} = -34 dB.

It may be noted how the high clutter case seriously reduced the probability of detection, even though the probability of false alarm is relatively high ($P_{FA} = 10^{-5}$) and the MTI clutter improvement factor is 48 dB.

There are conditions when the radar signal reflected from the target along the direct path may interfere with energy that assumes from the ray reflected from the ground (see Fig. 4). This can produce areas of varying signal strength which lead to regions of varying P_{DT}. The regions of low P_{DT} can cause missed target detections and loss of track. The detections effects of multipath depend upon antenna height, target height, target range, dielectric properties of the ground, surface roughness, the antenna pattern in the elevation plane and the wavelength. When the surface from which the indirect energy is reflected becomes rough, the specular multipath interference effect is decreased. However, diffuse multipath, which may look like noise, will increase as the reflecting surface becomes rougher.

On Fig. 5, the clutter was low. The curve labeled "rough surface" corresponds to rms height of surface irregularities σ_H = 5m and the curve labeled "smooth" corresponds to $\sigma_H = 0$.

On Fig. 6, the decrease in P_{DT} due to the combined effect of clutter and multipath is illustrated. The curve labeled "no clutter" corresponds to σ_{MED} = -54 dB and multipath effects are suppressed. The curve labeled "clutter" and multipath corresponds to σ_{MED} = 34 dB. It may be noted that multipath improver performance at some ranges but degrades it in others. The effects of multipath combined with clutter can make it difficult to establish and maintain target track

and discriminate between real targets and bird clutter.

On Fig. 7, surface is smooth and σ_{MED} = 34 dB. The difference in P_{DT} when the probability of false alarm varies from 10^{-5} to 10^{-6} is illustrated on Fig. 7. The primary effect of clutter is to require that the detection threshold be raised in order to keep P_{FA} within reasonable bounds. This demonstrates that the system will have to operate at false alarm rates higher than usual in order to maintain reasonable values of P_{DT}, thus requiring particular attention to be given to design of the tracker.

1. REFERENCES

1. Skolnik, M.I. (1970), "Radar Handbook", McGraw-Hill.

2. Fante, R., Franchi, P.R., Taylor, R.L. (1976), "Effects of Multipath on the Height-Finding Capabilities of a Fixed-Reflector Radar System," RADC-TR-76-163. AD# A027 661.

3. Fante, R.L. (1977), "Detection of Targets in Noise and Clutter", RADC-TR-77-243. AD# A047 535.

4. Lance, G.N. (1960), Numerical Methods for High Speed Computers", London.

5. Morrison, N. (1969), "Introduction to Sequential Smoothing and Prediction, McGraw-Hill.

6. Barton, D.K. (1964), "Radar Systems Analysis", Prentice-Hall.

ANALYSIS GEOMETRY

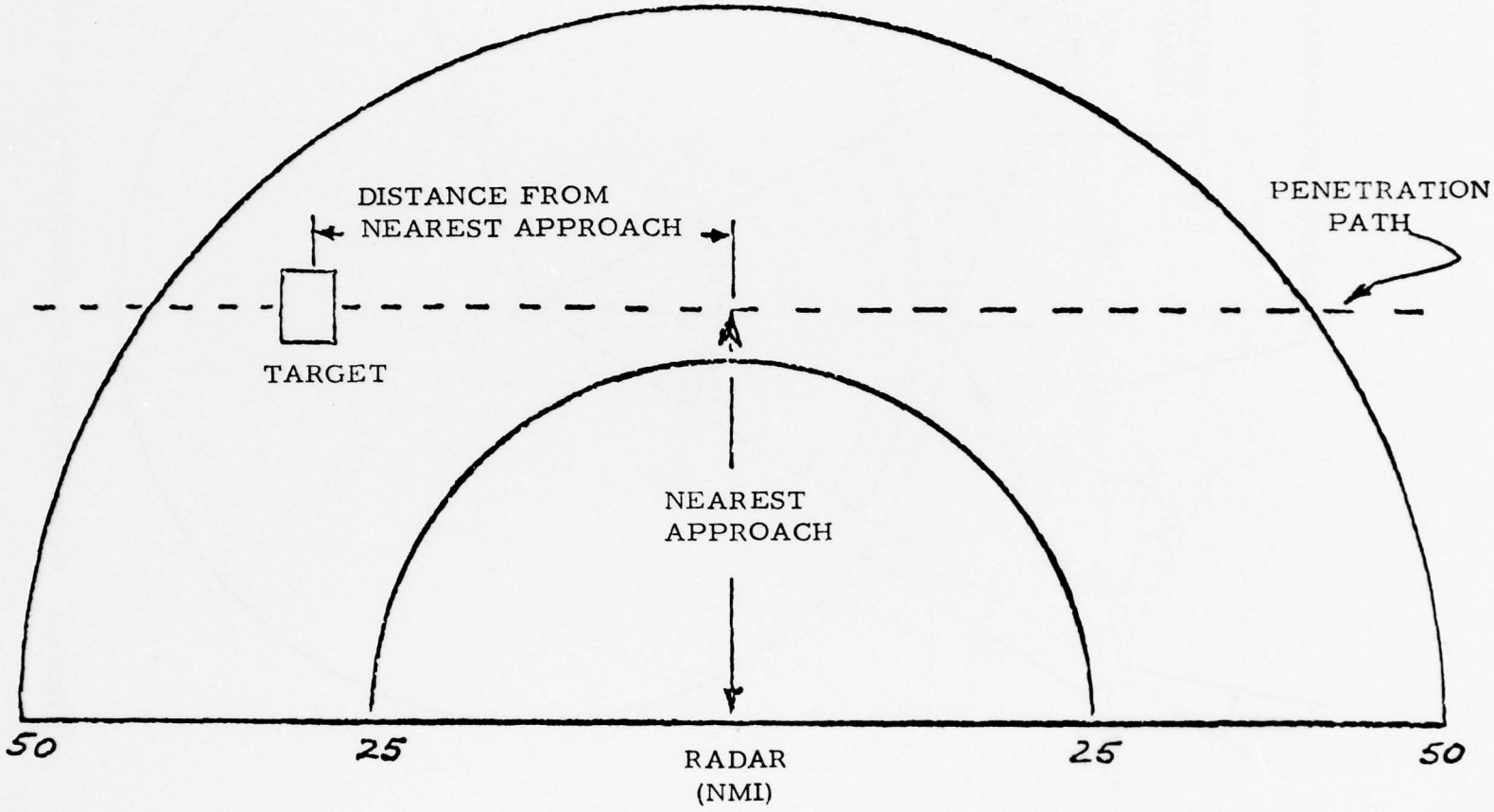

Fig. 1

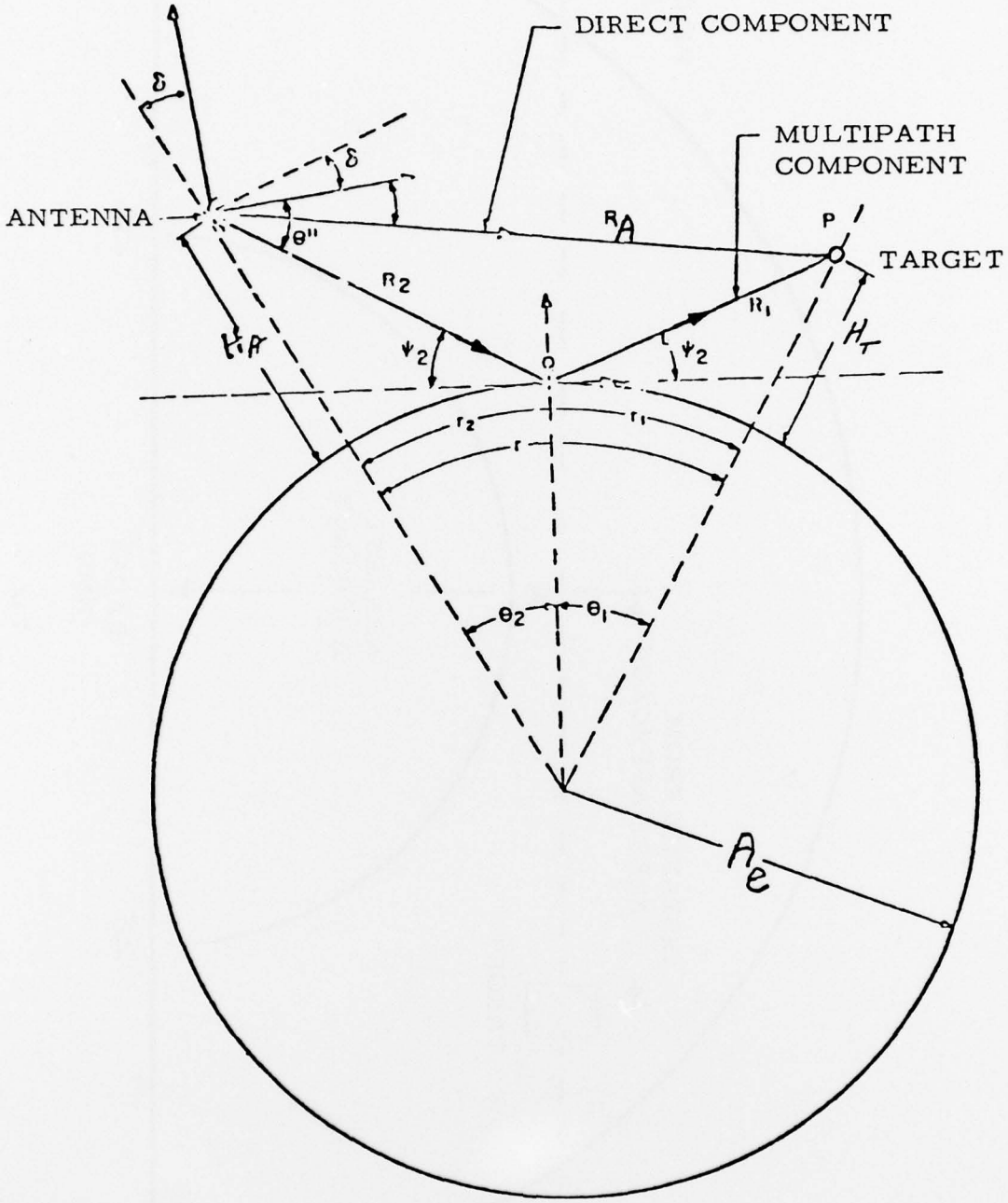

Figure 2. Geometry Used for Calculating the Multipath Effects

EFFECT OF CLUTTER ON P_{DT}

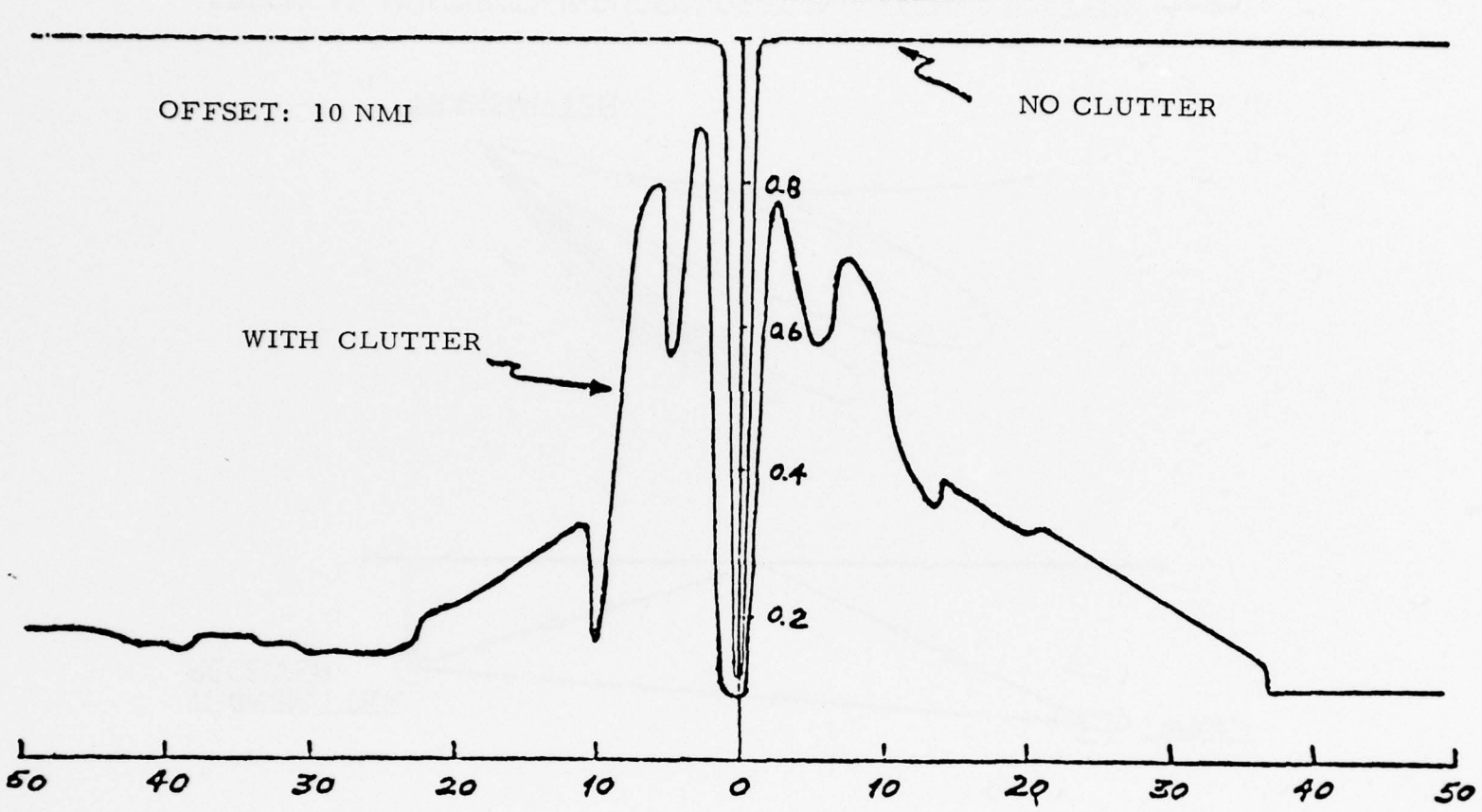

Fig. 3

SMOOTH EARTH → SPECULAR REFLECTION MULTPATH

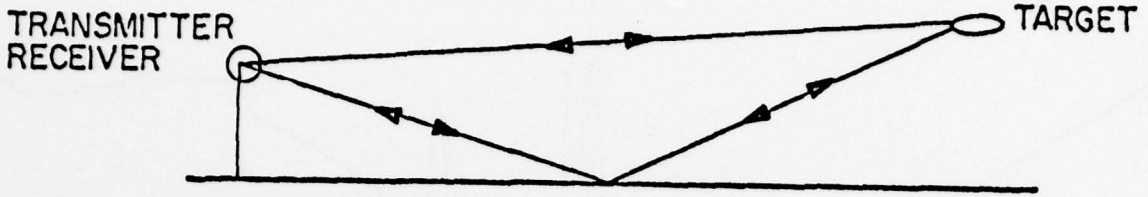

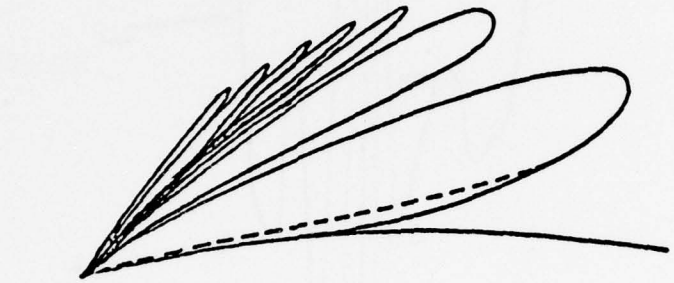

SPECULAR MULTIPATH INDUCES LOBES IN ANTENNA PATTERN → MISSED DETECTIONS & LOSS OF TRACK

Fig. 4

MULTIPATH EFFECTS

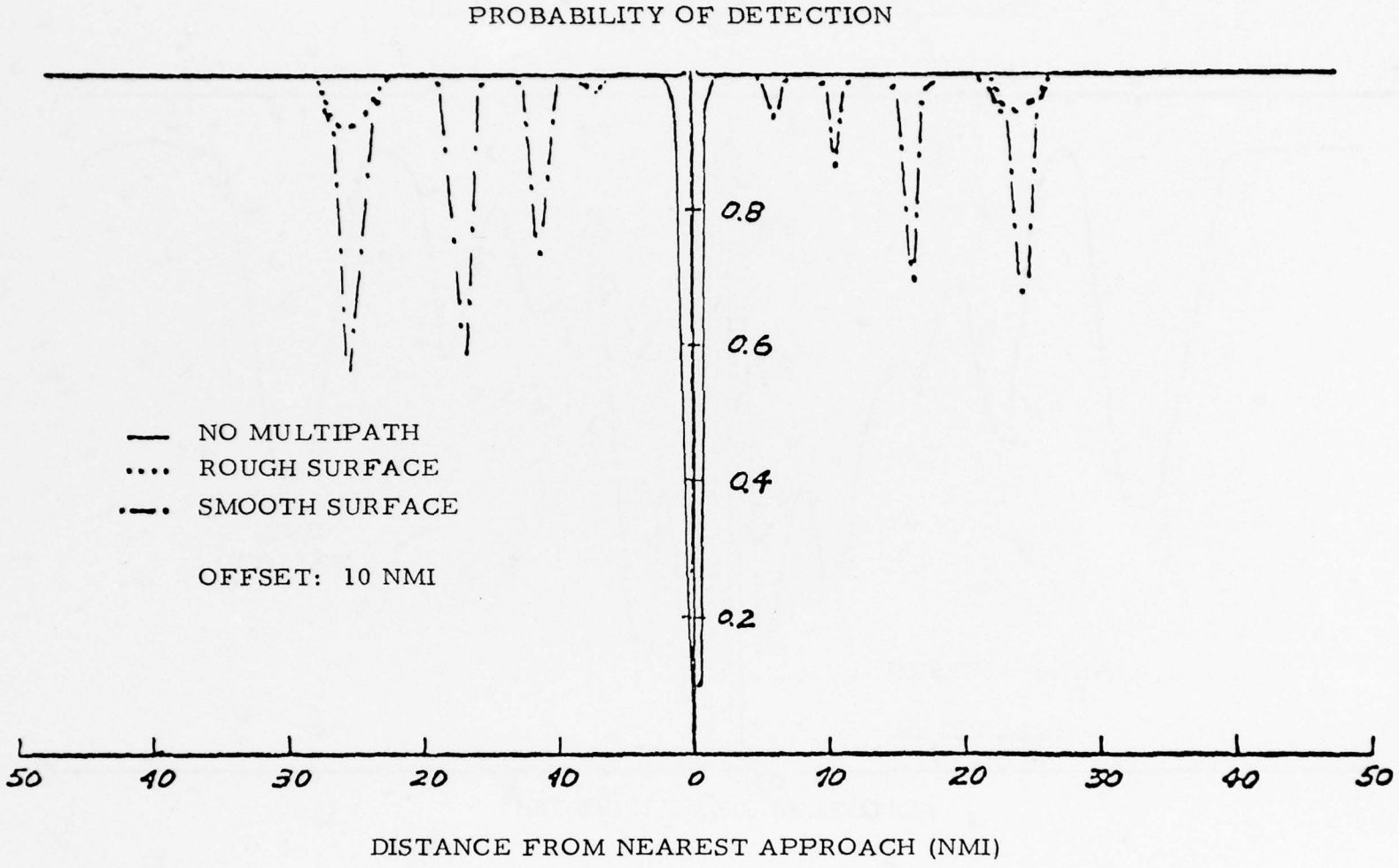

Fig. 5

EFFECT OF CLUTTER AND MULTIPATH ON P_{DT}

ROUGH SURFACE

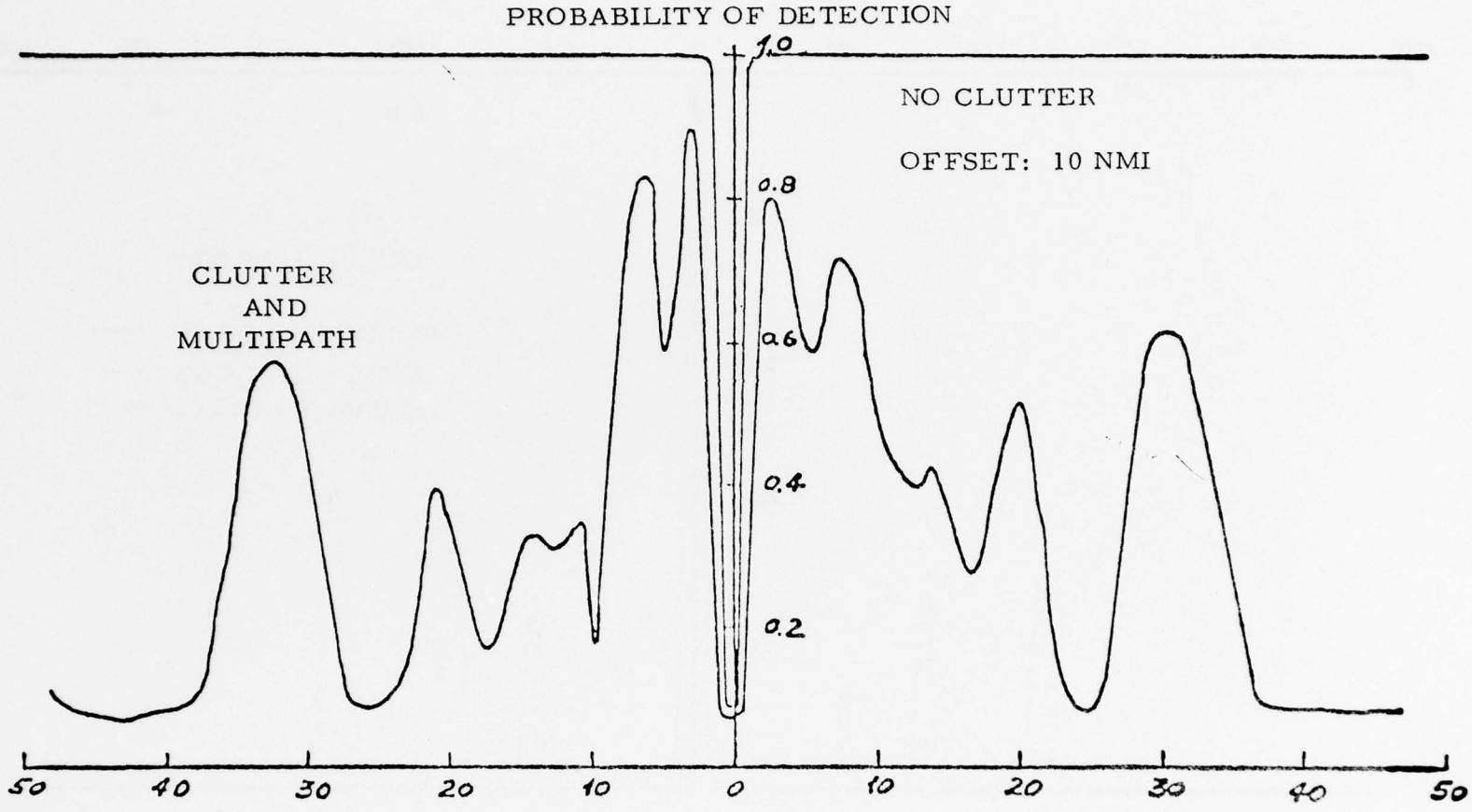

Fig. 6

MISSION
of
Rome Air Development Center

RADC plans and executes research, development, test and selected acquisition programs in support of Command, Control Communications and Intelligence (C^3I) activities. Technical and engineering support within areas of technical competence is provided to ESD Program Offices (POs) and other ESD elements. The principal technical mission areas are communications, electromagnetic guidance and control, surveillance of ground and aerospace objects, intelligence data collection and handling, information system technology, ionospheric propagation, solid state sciences, microwave physics and electronic reliability, maintainability and compatibility.

Printed by
United States Air Force
Hanscom AFB, Mass. 01731